SULPHUR-CONTAINING HAC EXPOSURE ON BETA CELL FUNCTION

EFFECT OF EXPOSURE TO SULPHUR-CONTAINING HETEROCYCLIC AROMATIC COMPOUNDS ON BETA CELL FUNCTION

By INELI PERERA, B.Sc.

A Thesis Submitted to the School of Graduate Studies in Partial Fulfilment of the Requirements

for the Degree Master of Science

McMaster University MASTER OF SCIENCE (2020) Hamilton, Ontario (Medical Sciences)

TITLE: Effect of Exposure to Sulphur-containing Heterocyclic Aromatic Compounds on Beta Cell Function AUTHOR: Ineli Perera, B.Sc. (University of Guelph) SUPERVISOR: Professor A.C. Holloway NUMBER OF PAGES: xiii, 70

LAY ABSTRACT

Non-occupational exposure to various environmental pollutants can contribute to the development of type 2 diabetes. The primary objective of this project was to explore a specific class of environmental pollutants commonly found in oil extraction sites. This thesis explores whether exposure to these pollutants can impair important functions in the beta cells, the cells in one's pancreas which secrete insulin in the body and regulate blood glucose levels, and whether these pollutants can increase one's risk of developing type 2 diabetes. The results of this thesis demonstrated that these pollutants may generate various types of cellular stress in the beta cell. Induction of cellular stress may impair the ability of beta cells to function normally. It is impaired beta cell function that leads to type 2 diabetes development. Therefore, the findings from this thesis may help further strengthen the association between environmental pollutant exposure and type 2 diabetes risk.

ABSTRACT

Type 2 diabetes (T2D) is characterized by impaired beta cell function. The generation of various types of cellular stresses, including oxidative stress and ER stress, and the induction of cellular senescence can contribute to beta cell dysfunction. Recent studies have demonstrated associations between petrochemical exposure and beta cell dysfunction, particularly through induction of cellular stress. One class of compounds, commonly found in crude oil, are sulphur-containing heterocyclic aromatic compounds (S-HACs). S-HACs have been previously demonstrated to induce cellular stress in mammalian cells. This thesis aims to determine if S-HACs can induce cellular stress in beta cells and, consequently, impair beta cell function, particularly insulin production.

Rat pancreatic beta cells, INS-1Es, were treated with two commonly occurring S-HACs, BNT(2,3D) and DBT, at doses which reflect non-occupational exposure levels. Upon treatment, various functional assays and qPCR experiments were performed for examining glucose uptake, ROS production, cellular senescence, ER stress and intracellular insulin production. It was observed that both BNT(2,3D) and DBT significantly increased glucose uptake and ROS production in the beta cells and upregulated the mRNA expression of various ER stress markers. In addition, BNT(2,3D) also induced cellular senescence, likely through a p53-independent pathway. This suggests that S-HACs may induce oxidative stress and ER stress in exposed beta cells, and some S-HACs may cause irreversible cell cycle arrest in response to these cellular stresses. However, intracellular insulin content in the INS-1Es was not altered by exposure to either S-HAC, suggesting that S-HACs may not impair insulin production. Nevertheless, the significant accumulation of ROS in S-HAC-exposed beta cells and the subsequent induction of cellular senescence by some S-HACs may alter other important beta cell functions, including

mitochondrial function and insulin secretion, which could lead to the development of T2D; suggesting the potential for S-HACs to be novel beta cell toxicants.

ACKNOWLEDGEMENTS

First and foremost, I would like to thank my supervisor Dr. Alison Holloway. You are an incredible and inspiring mentor. Thank you for believing in me and for teaching me the skills necessary to be a good scientific writer and researcher. I have become a much stronger and more confidant researcher because of you. I also wish to thank my committee members Dr. Sandeep Raha and Dr. Geoff Werstuck for their valued guidance through the course of this project. Your input has greatly shaped the direction of this project. I would also like to kindly thank Dr. Philippe Thomas for his valued input and assistance which has greatly impacted this project.

These past two years would not have been this fun and memorable without my amazing lab mates Ahmed Ayyash, Annia Martinez, Geemitha Ratnayake, Genevieve Perono, Laiba Jamshed, Lina Yacoub, Rob Gutgesell, Shanza Jamshed, Sergio Raez Villanueva and Simmy Joneja; as well as our fellow lab neighbours Anna Leonova and Shay Freger. Thank you for our daily lunch table talks and for all the wonderful adventures we embarked on together. I grew and learned many new skills as a young scientist because of my lab family. I am grateful to have been surrounded by such talented and knowledgeable young researchers!

I also want to thank my awesome best friends Polly and Rebecca. Thank you for providing the motivation and guidance needed to keep me on my feet. The late-night phone calls and video chats truly kept me going. Most importantly, I want to thank my amazing mom and dad and my sister Geshini. Their continued love and support enabled me to pursue the goals I set for myself and brought me to where I am today; and for that I am eternally grateful. Thank you for always being there for me. I love you very much.

TABLE OF CONTENTS

LIST OF FIGURES

LIST OF APPENDICES

LIST OF ABBREVIATIONS

2h-PG	2-hour plasma glucose levels
μM	Micromolar
γ-H2AX	Gamma-H2AX
A1C	Glycated hemoglobin level
ADP	Adenosine diphosphate
AGE	Advanced glycation end products
ATP	Adenosine triphosphate
BNT(2,3D)	Benzo[b]naphtho[2,3D]thiophene
Ca^{2+}	Calcium
cDNA	Complementary DNA
CT	Cycle threshold
DBT	Dibenzothiophene
ER	Endoplasmic reticulum
GPX	Glutathione peroxidase
HAC	Heterocyclic aromatic compound
IL	Interleukin
K_{ATP}	ATP sensitive potassium channel
mRNA	Messenger RNA
nM	Nanomolar
P300 HAT	p300 histone acetyltransferase enzyme
PAC	Polycyclic aromatic compound
pM	Picomolar
qPCR	Quantitative polymerase chain reaction
RAGE	AGE-specific receptor
Rb	Retinoblastoma proteins
ROS	Reactive oxygen species
SA-β Gal	Senescence-associated beta galactosidase enzyme

SASP	Senescence-associated secretory phenotype
S-HAC	Sulphur-containing heterocyclic aromatic compound
SOD2	Mitochondrial superoxide dismutase
T2D	Type 2 diabetes
TCDD	2,3,7,8-tetrachlorodibenzo-p-dioxin
UPR	Unfolded protein response

DECLARATION OF ACADEMIC ACHIEVEMENT

I, Ineli Perera, as the author of this Master's thesis paper wish to declare my research contributions to this thesis project, completed July 2020. Alongside completing all written work in this paper, I have conducted all experiments performed through the course of this project and have analyzed and appropriately presented all obtained results in this paper.

CHAPTER 1 – INTRODUCTION

1.1 TYPE 2 DIABETES MELLITUS

1.1.1 Prevalence

One of the most common metabolic diseases worldwide is diabetes mellitus which affects approximately 463 million people globally; with prevalence rates expected to increase by over 50% in the next 25 years (IDF 2019). Approximately 9% of the Canadian population currently has diabetes, however this is expected to rise to 12% within the next few years (Houlden 2018). Diabetes is classified into type 1, type 2, and gestational diabetes mellitus (Public Health Agency of Canada 2019). The most prevalent form of diabetes mellitus is type 2 diabetes mellitus (T2D), which makes up 90% of all cases in Canada (Public Health Agency of Canada 2019). In Canada, T2D is more prevalent in males, older adults and in certain populations including the Indigenous People of Canada (Houlden 2018; Public Health Agency of Canada 2019).

T2D is a leading contributor to premature mortality worldwide, alongside hypertension and tobacco use (Houlden, 2018). In 2008 and 2009, 1 in 10 deaths in Canada were due to complications from T2D, illustrating a strong association between diabetes and premature death (Houlden 2018).

1.1.2 Pathophysiology of T2D

T2D is characterized by impaired insulin secretion, systemic insulin resistance and impaired glucose tolerance (Cersosimo et al. 2018). In T2D, pancreatic insulin synthesis/production is not completely absent and therefore T2D patients generally do not require insulin therapy (Seino et al. 2010). Hence, T2D is often referred to as insulin-independent diabetes mellitus (Hameed et al. 2015). Various diagnostic tests exist for diagnosing prediabetes and T2D including

measurement of fasting plasma glucose in individuals who have fasted for at least 8 hours, measurement of glycated hemoglobin (A1C), and measurement of 2-hour plasma glucose levels (2h-PG) through an oral glucose tolerance test using 75g of glucose (Punthakee et al. 2018). Individuals diagnosed with prediabetes have a 2h-PG within the 7.8 mmol/L – 11.0 mmol/L range, fasting plasma glucose level within the 6.1 mmol/L – 6.9 mmol/L range, or an A1C level within the 6% - 6.4% range (Punthakee et al. 2018). Prediabetes, which is reversible, significantly increases an individual's risk of developing T2D, which is almost impossible to reverse (Punthakee et al. 2018). Individuals are diagnosed with T2D if they have a 2h-PG ≥ 11.1 mmol/L, a fasting plasma glucose level ≥ 7.0 mmol/L or an A1C ≥ 6.5%; indicating impaired glucose tolerance (Punthakee et al. 2018).

Over 90% of T2D patients are overweight or obese (Punthakee et al. 2018). T2D is sometimes referred to as adult-onset diabetes, as it is generally diagnosed in individuals over the age of 25. However, as obesity rates amongst children and adolescents continue to rise, the incidence rate of T2D amongst these populations has also been increasing (Punthakee et al. 2018). Obese individuals produce higher quantities of proinflammatory proteins, nonesterified fatty acids and various hormones which contribute to the development of insulin resistance (Al-Goblan et al. 2014). Insulin resistance is a condition where there is insufficient insulin-mediated glucose uptake by insulin-sensitive tissues and an inability of insulin to suppress hepatic glucose production (Leahy 2005). While most obese and overweight individuals are insulin resistant, not all of them develop T2D (Al-Goblan et al. 2014). This is because the pancreatic islets of the non-diabetic, insulin-resistant individuals secrete sufficient insulin into the bloodstream to compensate for the reduced insulin sensitivity in target tissues (Al-Goblan et al. 2014). This

ensures adequate uptake of glucose by these tissues for ATP production and glycogen synthesis (Al-Goblan et al. 2014).

The transition from normal to impaired glucose tolerance occurs due to impaired insulin secretion in which the beta cells in the pancreas are unable to secrete sufficient quantities of insulin into the bloodstream to compensate for insulin resistance (Al-Goblan et al. 2014; Leahy 2005). Impaired insulin secretion by pancreatic beta cells characterizes beta cell dysfunction, which occurs in both prediabetes and T2D (Leahy 2005; Punthakee et al. 2018).

1.1.3 Functions of the Pancreatic Beta Cell

Pancreatic beta cells are insulin-secreting cells found in the Islets of Langerhans in the endocrine region of the pancreas (Skelin et al. 2010). The nutrient molecule glucose is a key regulator of various cellular processes in the beta cell including insulin synthesis and secretion (Skelin et al. 2010). A rise in blood glucose levels induces transcription of the insulin gene and, subsequently, production of the insulin precursor preproinsulin which is comprised of an A chain, B chain, C peptide and N-terminal signal peptide (Skelin et al. 2010). Attachment of the preproinsulin inside the endoplasmic reticulum cleaves the signal peptide off the molecule, converting preproinsulin into proinsulin (Skelin et al. 2010). Proinsulin is sent to the Golgi apparatus and packed into vesicles (Skelin et al. 2010). Within each vesicle proinsulin matures into insulin, through cleaving of the C peptide, and is stored in the beta cell until glucose-stimulated secretion (Skelin et al. 2010).

In healthy individuals, a rise in blood glucose concentrations leads to the cellular uptake of glucose into beta cells through the GLUT2 transporter proteins embedded in the cellular membrane, as shown in Appendix 1 (Skelin et al. 2010). Upon entering the beta cell, glucose is

phosphorylated by glucokinase and undergoes glycolysis to generate pyruvate (Fridlyand & Philipson 2011). Pyruvate enters the tricarboxylic acid cycle and generates the reducing equivalents NADH and FADH2 (Fridlyand & Philipson 2011). These coenzymes donate electrons to the electron transport chain located in the inner mitochondrial membrane (Fridlyand & Philipson 2011). This generates an electrochemical gradient that drives the production of ATP (Fridlyand & Philipson 2011). Increased ATP:ADP concentrations in the cytosol cause ATP-sensitive K^+ (K_{ATP}) channels in the cell's plasma membrane to close and plasma membrane depolarization to occur (Fridlyand & Philipson 2011). This triggers the opening of voltage gated calcium channels, resulting in a Ca^{2+} influx (Fridlyand & Philipson 2011). Increased Ca^{2+} concentrations in the cytosol stimulates the release of vesicle-stored insulin out of the cell and into the bloodstream (Skelin et al. 2010).

Insulin secretion occurs in a pulsatile manner and consists of two phases (Leahy 2005). The first phase of insulin secretion is short and occurs immediately upon high caloric intake. The second phase is much longer and proceeds until blood glucose levels return to normoglycemic conditions (Leahy 2005). While the secretion of insulin by beta cells is stimulated by hyperglycemia, the secretion of glucagon into the bloodstream by pancreatic alpha cells, also located in the Islets of Langerhans, is inhibited (Cersosimo et al. 2018). Glucagon functions to increase blood glucose levels during fasting states (Cersosimo et al. 2018). Hyperglycemia significantly increases the ratio of plasma insulin to plasma glucagon concentrations and this suppresses gluconeogenic and glycogenolytic processes in the liver (Cersosimo et al. 2018). The elevated levels of insulin also trigger glucose uptake by the liver and, upon entering the peripheral veins, triggers glucose uptake by peripheral insulin-dependent tissues, including

muscle and adipose tissue (Cersosimo et al. 2018). Glucose uptake into these target tissues stimulates glycogen synthesis, thereby promoting glucose homeostasis (Cersosimo et al. 2018).

1.2 PATHWAYS TO IMPAIRED BETA CELL FUNCTION

Beta cell dysfunction is a key characteristic of T2D (Hasnain et al. 2016). While there are a number of pathways which have been shown to contribute to beta cell dysfunction the generation of cellular stress, including oxidative stress and endoplasmic reticulum stress, have consistently been shown to lead to impaired beta cell function (Hasnain et al. 2016).

1.2.1 Oxidative Stress and Cellular Senescence

Oxidative phosphorylation in the mitochondria, which occurs as a result of glycolysis, generates ATP through the conversion of oxygen to water via the electron transport chain (Kasai et al. 2020). Some of these oxygen molecules, however, can escape the electron transport chain and be reduced to the reactive superoxide anion radical O_2^- (see Appendix 2) (Kasai et al. 2020). An increase in superoxide concentrations within the mitochondria triggers the mitochondrial superoxide dismutase (SOD2) to convert the superoxide anions to O_2 and H_2O_2 (Kasai et al. 2020). The H_2O_2 may then be converted to H_2O by glutathione peroxidase (GPX) or to H_2O and O_2 by catalase (Kasai et al. 2020). However, H_2O_2 may also be reduced to the extremely reactive hydroxyl radical by free iron, which can be released into the mitochondrial environment through inactivation of iron-rich enzymes by the superoxide anions (Kasai et al. 2020). The production of reactive oxygen species (ROS) in the mitochondria such as O_2^- and hydroxyl radicals leads to the activation of NRF2 (Kasai et al. 2020). Activated NRF2 translocates to the nucleus where it induces the transcriptional activation of genes encoding various antioxidant enzymes including *SOD2*, *CATALASE* and *GPX* (Kasai et al. 2020).

With persistent hyperglycemia, excess glucose uptake and metabolism by beta cells may lead to the accumulation of ROS (Drews et al. 2010). Pancreatic beta cells, in comparison to other cell types in the body, have low expression of antioxidant enzymes including superoxide dismutase (Drews et al. 2010). Poor antioxidant defence mechanisms combined with excess generation of ROS can lead to oxidative damage of DNA in beta cells (Drews et al. 2010).

Cellular repair mechanisms are activated in response to oxidative DNA damage (Barnes 2015). For example, DNA damage activates the tumour suppressor pathway comprised of the proteins P53 and P21 (see Appendix 3) (Barnes 2015). Activation of the transcription factor P53 upregulates the expression of the *P21* gene (Barnes 2015). P21 protein binds to and inhibits cyclin dependent kinases which normally function to phosphorylate and inactivate retinoblastoma (Rb) proteins, the major regulator of the G1/S checkpoint in the cell cycle (Rincheval et al. 2002). The active, dephosphorylated Rb proteins irreversibly arrest the cell cycle at the G1 phase (Rincheval et al. 2002). This permanent non-proliferative state is known as cell senescence (Barnes 2015).

1.2.2 Characteristic Features of Senescent Cells

Senescent cells have been observed to express high levels of BCL2, an anti-apoptotic protein that can also inhibit cell proliferation (Rincheval et al. 2002). Alongside inducing cell senescence, activation of P53 can also induce apoptosis through upregulating the expression of proapoptotic proteins such as BAX (Rincheval et al. 2002). It has been suggested that the ratio of BCL2:BAX proteins expressed in cells may determine whether a cell enters an apoptotic state or a senescent state, upon activation of P53 (Rincheval et al. 2002). Interestingly, upregulation in BCL2 expression has been shown to promote P53-dependent senescence, through transforming cells in an apoptotic state to a senescent state at the G2 phase of the cell cycle (Rincheval et al.

2002). This suggests a potential role of anti-apoptotic proteins in promoting cell senescence (Rincheval et al. 2002).

A key feature of senescent cells that distinguish them from proliferating cells is an increased expression of the senescence-associated beta galactosidase enzyme (SA-β GAL), encoded by the *GLB1* gene (Lee et al. 2006). Neither the functional role of SA-β GAL in cell senescence nor the mechanistic pathway through which this enzyme is expressed are currently known (Lee et al. 2006). However, it has been suggested that increased SA-β GAL activity in senescent cells may be occurring due to increased lysosomal β-galactosidase activity (Lee et al. 2006). Lysosomal β-galactosidase, also encoded by the *GLB1* gene, is solely found in the lysosomes of mammalian cells (van der Spoel et al. 2000). Lysosomal β-galactosidase hydrolyzes β-galactosides from glycoproteins and keratan sulfate (van der Spoel et al. 2000); lysosome content has been observed to be significantly higher in senescent cells (Lee et al. 2006).

Cell cycle arrest prevents the accumulation of damaged beta cells, but at the same time accelerates the aging of these cells (Barnes 2015). The senescent beta cells, despite being non-proliferative, are metabolically active (Barnes 2015). They begin to secrete inflammatory chemokines and cytokines such as IL6, IL1β and CCL2 (MCP1) (Barnes 2015), as well as profibrotic proteins such as PAI1 (SERPINE1) (Khan et al. 2017). This inflammatory response occurs due to NFkB activation subsequent to P21 activation and is known as a senescence-associated secretory phenotype (SASP) (Barnes 2015). SASP amplifies the degree of senescence within the cell and induces senescence in neighbouring cells which will in turn lead to premature aging of pancreatic islets which is linked to T2D (Barnes 2015).

1.2.3 Cellular Senescence and Impaired Beta Cell Function

Increased production of SASP markers, such as IL1β and IL6, has been observed in pancreatic islets of T2D patients (Larsen et al. 2007) and that increased production of IL1β in beta cells reduces the maturation of proinsulin to insulin in the beta cells (Larsen et al. 2007). Furthermore, increased IL1β production and secretion in pancreatic islets upregulates FAS expression (Choi et al. 2009); the FAS receptor is known to regulate cell apoptosis. In addition, recent studies have shown that this cell surface receptor can also regulate the insulin exocytosis machinery (Choi et al. 2009; Schumann et al. 2007). There are a number of proteins involved in insulin vesicle exocytosis, the most crucial of which are SNARE proteins (Xiong et al. 2017). SNARE proteins assemble into a complex that aids in fusing the insulin secretory vesicles with the cell's plasma membrane in order to subsequently release the vesicle contents (i.e. insulin) into the bloodstream (Xiong et al. 2017). Absence of *FAS* gene significantly improves insulin exocytosis, in part due to increased expression of SNARE proteins, such as VAMP2 and syntaxin-1A, and increased expression of munc18a which regulates the assembly of the SNARE proteins (Choi et al. 2009). Therefore, upregulation in FAS expression, as a result of increased IL1β production, may impair insulin exocytosis and raise fasting plasma glucose concentrations (Choi et al. 2009; Larsen et al. 2007).

Plasma concentrations of the SASP marker IL6 are also increased systemically in T2D individuals (Akbari & Hassan-Zadeh 2018). Increased systemic production of the IL6 protein has been shown to induce insulin resistance in certain insulin-sensitive tissues, such as adipose tissue and the liver, by reducing the phosphorylation of insulin receptor substrates (Akbari & Hassan-Zadeh 2018). As previously mentioned, insulin resistance is regarded as the first condition observed in the pathogenesis of T2D that can lead to beta cell dysfunction. Interestingly,

prolonged exposure of human pancreatic islets to IL6 significantly reduces glucose-stimulated insulin secretion (Ellingsgaard et al. 2008). Thus, persistent production of IL6 by pancreatic beta cells, and systemic production of this cytokine by other tissues, may contribute to the development of T2D by inducing insulin resistance and impairing beta cell function.

1.2.4 ER Stress and the Unfolded Protein Response

Alongside increased mitochondrial ROS production, impaired protein homeostasis in the endoplasmic reticulum can also contribute to T2D development (Eizirik et al. 2007). The endoplasmic reticulum (ER) is central to the synthesis, folding and posttranslational modification of proteins, including insulin (Pluquet et al. 2014). During hyperglycemic conditions, increased uptake of glucose increases the demand for beta cells to synthesize and secrete more insulin (Burgos-Moron et al. 2019). Increased insulin synthesis increases the presence of unfolded proteins in the ER (Burgos-Moron et al. 2019). Accumulation and aggregation of these unfolded proteins generates ER stress (Eizirik et al. 2007). Therefore, exposure to hyperglycemic conditions makes beta cells highly prone to ER stress (Burgos-Moron et al. 2019).

Furthermore, protein folding involves the formation of disulphide bonds which stabilize the folded proteins (Pluquet et al. 2014). The ERO1 enzyme builds these disulphide bonds with the use of oxygen (Pluquet et al. 2014). However, disulfide bond formation can generate ROS, particularly H_2O_2 which can diffuse freely across various compartments within the cell (Pluquet et al. 2014). The generation of ROS through disulphide bond formation in the ER, as well as through mitochondrial oxidative phosphorylation, can also trigger accumulation of unfolded proteins in the ER and thereby sustain, rather than attenuate, ER stress conditions (Burgos-Moron et al. 2019).

Various mechanisms within the ER exist to detect and eliminate unfolded proteins (Pluquet et al. 2014). The primary mechanism induced by ER stress is the unfolded protein response (UPR) (Pluquet et al. 2014). UPR is initiated by the dissociation of ER chaperone GRP78 from the transmembrane proteins IRE1, PERK and ATF6 such that GRP78 can bind to unfolded proteins (Bhandary et al. 2013). GRP78 dissociation leads to the activation of the three transmembrane proteins, inducing signalling pathways which slow the rate of protein synthesis and upregulate the expression of genes encoding important protein folding chaperones, including GRP78, and genes associated with the removal and degradation of misfolded proteins (Pluquet et al. 2014). UPR can also activate proinflammatory proteins such as TXNIP, and proapoptotic proteins such as CHOP (Pluquet et al. 2014). A detailed illustration of these pathways is presented in Appendix 4.

1.2.5 RAGE - Linking ER Stress with Senescence

During hyperglycemic conditions, glucose can modify proteins to generate advanced glycation end products (AGE) (Piperi et al. 2012). The production and accumulation of AGE can damage the structure of proteins and impair their function (Piperi et al. 2012). AGE can exert their effects on the cell by binding to the AGE-specific receptor (RAGE) embedded within the cell membrane (Piperi et al. 2012). Binding to RAGE activates various signalling pathways including pathways which induce ROS production (Piperi et al. 2012). It has been observed that exposing beta cells to AGEs not only increases mitochondrial ROS production, but as well it can increase glucose uptake into the beta cell, reduce ATP production and impair insulin secretion (Coughlan et al. 2011). Various studies have also demonstrated that AGE exposure can directly induce ER stress in mammalian cells (Piperi et al. 2012). Induction of ER stress, and the

subsequent UPR, by AGE can activate p21 signalling and induce cellular senescence (Liu et al. 2014).

1.2.6 The Unfolded Protein Response and Impaired Beta Cell Function

In its attempt to reduce the accumulation of unfolded proteins and alleviate ER stress, the unfolded protein response may further impair beta cell health and induce beta cell dysfunction (Kim et al. 2012). For example, activation of the PERK pathway, through disassociation of GRP78 from PERK, induces phosphorylation of the initiation factor eIF2α (Back et al. 2009). This consequently attenuates the synthesis of proinsulin (Back et al. 2009). GRP78 also dissociates from and activates IRE1 which induces splicing of *XBP1* mRNA leading to increased expression of the XBP1 protein, a transcription factor which increases protein folding and promotes degradation of misfolded proteins (Kim et al. 2012). Overexpression of XBP1 protein can downregulate mRNA expression of *MAFA* and *PDX1*, important regulators of insulin gene expression, and induce insulin mRNA degradation, thereby leading to reduced insulin mRNA expression (Kim et al. 2012). Alongside this, prolonged activation of the ATF6 pathway can also decrease *MAFA* and *PDX1* gene expression and impair the ability of these transcription factors to induce insulin transcription (Kim et al. 2012). Interestingly, activation of ATF6 also increases the expression of the nuclear receptor small heterodimer partner (Kim et al. 2012). The small heterodimer partner protein has been shown to downregulate the biosynthesis and secretion of insulin, likely by suppressing the activity of BETA2, a transcription factor which normally upregulates insulin gene expression (Kim et al. 2012). Therefore, activation of UPR, due to ER stress, can downregulate insulin gene expression and impair insulin biosynthesis leading to reduced glucose-stimulated insulin secretion and beta cell dysfunction (Kim et al. 2012; Eizirik et al. 2007).

1.3 FACTORS ASSOCIATED WITH T2D DEVELOPMENT

1.3.1 Lifestyle and Genetic Factors

Various factors are associated with the development of T2D (Wu et al. 2014). Commonly known factors are lifestyle factors which include consuming a diet rich in fat and sugar and low in fibre and being physically inactive (Wu et al. 2014). Habits such as high alcohol consumption and frequent use of nicotine-containing products have also been associated with T2D development (Wu et al. 2014). Alongside lifestyle choices, genetics may also be a contributing factor, with the incidence rate of diabetes being higher amongst first degree relatives of T2D individuals when compared to the incidence rate of diabetes in the general population (Wu et al. 2014).

1.3.2 Environmental Factors

In recent decades, a growing body of evidence has demonstrated that exposure to environmental pollutants may also contribute to the development of T2D (Fabricio et al. 2016). For example, dioxin (2,3,7,8 – tetrachlorodibenzo-p-dioxin; TCDD) which was used in previous decades as an herbicide, has been shown to decrease the rate of glucose uptake and increase the production of proinflammatory cytokines in beta cells which contribute to reduced insulin secretion (Fabricio et al. 2016). Furthermore, chronic exposure to TCDD can also exhaust beta cells and impair their ability to produce insulin by persistently inducing calcium influx into the cell and increasing the secretion of insulin from the cell (Fabricio et al. 2016). TCDD is classified as a persistent organic pollutant due to its ability to bioaccumulate in host organisms and the environment (Hectors et al. 2011). It is one of the most toxic persistent organic pollutants currently known (Fabricio et al. 2016).

Another class of persistent organic pollutants are heterocyclic aromatic compounds (HACs) (Net al. 2015). These are organic compounds containing multiple conjugated rings into which may be embedded oxygen, nitrogen, or sulphur atoms (Li et al. 2014). Many studies have demonstrated a positive association between exposure to HAC-rich substances and diabetes. For example, it has been demonstrated that exposure to cigarette smoke, which is rich in HACs, can induce oxidative stress and ER stress in beta cells (Coggins et al. 2011; Tong et al. 2020). Furthermore, the generation of cellular stress was associated with reduced insulin gene expression and impaired insulin secretion in the beta cells exposed to cigarette smoke (Tong et al. 2020). Beta cell proliferation was also impaired by cigarette smoke exposure, likely due to reduced protein expression of the cell cycle regulator CYCLIN D2 (Tong et al. 2020). Therefore, exposure to cigarette smoke affects various pathways and components of beta cell health and function, and HACs may be a prime contributor to these effects.

1.4 HETEROCYCLIC AROMATIC COMPOUNDS (HACs)

1.4.1 HACs in Bitumen and Crude Oil

Certain HACs such as dibenzofuran and dibenzothiophene are commonly found in crude oil (Asif & Wenger 2019). Crude oil is a refined product of bitumen, a dark highly viscous liquid extracted from bitumen-rich sands, known as oil sands (Yoon et al. 2009). Alberta contains one of the largest oil sands deposits in the world; estimated to generate close to 1.8 trillion barrels of bitumen (Li et al. 2014). The oil sands are situated in the Peace River, Cold Lake and Athabasca regions in Alberta (Li et al. 2014). The chemical composition of the bitumen can vary between oil sand regions and this can affect the quality of the extracted bitumen and its refined crude oil products (Yoon et al. 2009). On a molecular scale, bitumen is comprised primarily of aromatic

compounds, while on an elemental scale, the aromatic compounds in bitumen are comprised primarily of carbon and hydrogen atoms with traces of nitrogen, oxygen and sulphur (Yoon et al. 2009). Interestingly, the concentration of sulphur in bitumen extracted from the Athabasca region is substantially higher than that of bitumen extracts from other oil sands regions (Yoon et al. 2009).

1.4.2 Routes of Exposure

HACs may enter the body through ingestion, inhalation, or dermal exposure (Lin et al. 2016). Individuals in both occupational and non-occupational settings can be exposed to HACs through inhalation of emissions and fumes generated from the combustion of gasoline, diesel and coal (Abdel-Shafy & Mansour 2016). Furthermore, individuals can also be exposed to HACs through dermal contact and ingestion (Eisentraeger et al. 2008). This may be due to the presence of HACs in soils, sediments and freshwater sources, such as groundwater, that may have become contaminated as a result of accidental chemical spills or seepage from oil refineries and other industrial sites (Eisentraeger et al. 2008). HACs have also been found in certain grilled and cooked meats, as well as in fish collected from water bodies previously contaminated by oil spills (IARC 2013).

1.4.3 Crude Oil and T2D

Diesel exhaust is a combustion product of diesel fuel, which is a refined product of crude oil (Williams et al. 1986). Exposure of the rat beta cell lines INS-1 and RIN-m5F to diesel exhaust particulates, significantly increased ROS production and P53 protein expression, and induced DNA damage (Du et al. 2019). Furthermore, diesel exhaust exposure significantly reduced intracellular ATP production and insulin secretion rates in the treated beta cells (Du et al. 2019).

In healthy beta cells, increased cytosolic ATP concentrations drive insulin secretion (Du et al. 2019). Therefore, constituents in diesel exhaust are capable of increasing ROS production and inducing oxidative DNA damage in pancreatic beta cells, leading to reduced ATP synthesis and, consequently, impaired insulin exocytosis (Du et al. 2019).

In a similar study, it was observed that exposure to diesel exhaust particles significantly upregulated mRNA and protein expression of RAGE in human and rat alveolar epithelial cells (Reynolds et al. 2011). It was also observed that diesel exhaust particulates activated NFkB and induced the secretion of the inflammatory proteins MCP1 and IL8 (Reynolds et al. 2011). Induction of an inflammatory response by diesel exhaust particulates suggests that constituents of the diesel exhaust mixture may be RAGE ligands, which can activate RAGE and induce an inflammatory response similar to the SASP expressed in senescent cells (Reynolds et al. 2011). As previously discussed, activation of RAGE can induce cellular senescence through generating ER stress (Liu et al. 2014). Therefore, diesel exhaust constituents may generate ER stress and oxidative stress in pancreatic beta cells. The generation of cellular stress may impair beta cell function and induce cellular senescence.

1.5 SULPHUR-CONTAINING HETEROCYCLIC AROMATIC COMPOUNDS (S-HACs)

1.5.1 S-HACs and Its Properties

Crude oil products, like diesel fuel, as well as bitumen itself contain high quantities of sulphur-containing HACs (S-HACs) which are HACs with a thiophene ring embedded within the compound (Jacob et al. 1986; Yang et al. 2016). The thiophene ring may be embedded either centrally or peripherally within the HAC (Jacob et al. 1991). S-HACs are metabolized by either one of two ways based on the location of the thiophene ring (Jacob et al. 1991). S-HACs with a

central thiophene ring are metabolized by sulphur-oxidation to generate sulfones and sulfoxides, while S-HACs with a peripherally located thiophene ring undergo oxidation at the benzene rings to generate compounds such as phenols (Jacob et al. 1991).

Two important S-HACs commonly found in crude oil and in bitumen are dibenzothiophene and benzo[b]naphtho-thiophene isomers (Yang et al. 2016). Despite the presence of these compounds in crude oil mixtures and in the environment, very little is known about the toxicological properties of these compounds (Jacob et al. 1991). Much of the toxicological research conducted on polycyclic aromatic compounds (PACs), the major class of aromatic compounds to which S-HACs and HACs belong to, has focused on polycyclic aromatic hydrocarbons which are also found in crude oil (Jacob et al. 1991). Existing studies on S-HACs examine the compound's carcinogenic potential (IARC Monographs 2013); however, the effects of S-HAC exposure on metabolic function remain poorly understood.

1.5.2 S-HAC Exposure and Induction of Cellular Stress

Interestingly, a 2017 study has shown that the naturally occurring S-HAC dibenzothiophene (DBT) may be a potent toxicant through examining the effects of DBT exposure on human neuroblastoma cells (Sarma et al. 2017). Several important observations were made. First, DBT significantly increased ROS levels in the neuroblastoma cells and significantly lowered the cell's mitochondrial membrane potential (Sarma et al. 2017). Mitochondrial membrane potential, generated during oxidative phosphorylation, is an important indicator of mitochondrial function (Zorova et al. 2018). Second, DBT significantly upregulated the expression of mitochondrial pro-apoptotic proteins as well as oxidative stress-responsive proteins (Sarma et al. 2017). Lastly, DBT significantly increased the concentration of the oxidative damage marker, hydroperoxidase (Sarma et al. 2017). This study therefore suggests that DBT can increase ROS levels in

mammalian cells. Furthermore, it demonstrates the ability of DBT to impair mitochondrial membrane potential to such an extent that it can induce oxidative damage in the cell and potentially cause cell death (Sarma et al. 2017). Since beta cells are highly prone to oxidative stress (Drews et al. 2010), DBT may potentially induce oxidative stress in the beta cells by increasing the production of mitochondrial ROS. Beta cells are also prone to ER stress (Burgos-Moron et al. 2019), and the accumulation of ROS by DBT may also generate ER stress.

Due to the ability of S-HAC rich products in inducing cellular stress in mammalian cells, it is therefore plausible that exposure to S-HACs may also induce oxidative stress and ER stress in pancreatic beta cells. This, in turn, may impair normal beta cell function, specifically insulin production and secretion.

1.6 HYPOTHESIS

This project will test the hypothesis that S-HACs negatively impact pancreatic beta cell health and function. We will specifically focus on benzo[b]naphtho[2,3d] thiophene (BNT(2,3D)) and dibenzothiophene (DBT) which are two naturally occurring S-HACs found in petroleum and bitumen (Mossner & Wise 1999). The goals of this study are to determine whether these S-HACs can induce oxidative stress and ER stress in beta cells and whether this, in turn, induces cellular senescence to cause premature beta cell aging. Additionally, and most importantly, we want to investigate whether insulin production is impaired by the cellular stress that may be induced by S-HAC exposure.

CHAPTER 2 – METHODS

2.1. OBJECTIVES

There are five main objectives in this project. The first objective is to determine whether exposure to BNT(2,3D) and DBT alters glucose uptake into the treated beta cells. The second objective is to determine whether these S-HACs induce oxidative stress, specifically ROS accumulation and impaired antioxidant activity. The third objective is to determine whether the S-HACs induce ER stress. The fourth objective is to determine whether the S-HACs cause cell cycle arrest and induce cell senescence. Lastly, and most importantly, the fifth objective is to determine whether BNT(2,3D) and DBT alter insulin production in the beta cell.

2.2. CELL MODEL AND CELL CULTURE MAINTENTANCE

To examine the potential effects of S-HACs on pancreatic beta cells, the rat insulinoma INS-1E cell line was chosen as the model system. INS-1E cells are clonal cells of their parent insulin-secreting cell line INS1 (Merglen et al. 2004). INS-1E cells are highly proliferative (Skelin et al. 2010) and, compared to their parent cell line, can be efficiently cultured up to 100 passages (Merglen et al. 2004). INS-1E cells express both GLUT2 protein, for glucose uptake, and glucokinase protein, for glucose metabolism (Skelin et al. 2010). Therefore, this cell line is responsive to glucose in a physiologically relevant range and generates a high quantity of insulin (Skelin et al. 2010).

INS-1E rat insulinoma cells, generously provided by Dr. Claes Wollheim (Geneva, Switzerland), were cultured in RPMI 1640 media supplemented with 10mM HEPES and 2mM L-glutamine (Corning, Virginia, USA) as well as 50μM 2-mercaptoethanol, 10% heat-inactivated fetal bovine serum (Hyclone, Utah, USA), 1mM sodium pyruvate (GIBCO, Burlington, Ontario),

1% penicillin and streptomycin (GIBCO, Burlington, Ontario) at 37°C and 5% CO_2 environment. Upon reaching 80% confluency, cells are passaged by first washing with Dulbecco's phosphate-buffered saline (DPBS) (Corning, Virginia, USA) and afterwards applying 1X trypsin with NaCl and EDTA onto the cells and incubating for 5 minutes at 37°C. Cells within passages 50-80 were used for all treatments and experiments.

2.3. TREATMENT COMPOUNDS

The S-HACs benzo[b]naphtho[2,3d]thiophene (BNT(2,3D)) (European Commission JRC, Geel, Belgium) and dibenzothiophene (DBT) (Toronto Research Chemicals, North York, Ontario) were chosen as the treatment compounds of interest; see Appendix 5. Stock solutions of BNT(2,3D) and DBT were prepared with DMSO as the vehicle solvent. The treatment doses used in the proceeding experiments ranged from 1pM to 10μM, depending on the outcome measure examined. Controls were treated with vehicle solvent DMSO at the highest concentration used for the S-HAC treatments for each outcome measure.

2.4. CYTOTOXICITY OF COMPOUNDS

To determine a suitable dose range that is not cytotoxic to the INS-1E cells, an MTS assay (Promega, Wisconsin, USA) was performed. INS-1E cells were seeded in a 96-well plate at seeding density of 200,000 cells/mL. Cells were cultured in media and treated with BNT(2,3D) and DBT at doses ranging from 1nM to 10μM, with a sample size of n=5 in duplicate. Treated cells were incubated for 48 hours at 37°C, after which MTS reagent (Promega, Wisconsin, USA) was applied and plate was incubated for 2 hours at 37°C. Afterwards, absorbance was read at 490nM in the Synergy H4 Hybrid microplate reader (BioTek Instruments, Vermont, USA).

With the obtained absorbance values the % cell viability was calculated for each sample of each treatment group by calculating the ratio of the number of live cells to the number of dead cells. Treatment doses not considered to be cytotoxic to the cell model have % cell viability values which are above 80% of the viability in vehicle-treated cells. This is the standard cell viability threshold in toxicology studies (López-García et al. 2014). The results from the MTS assay indicated that all doses below 10μM for both BNT(2,3D) and DBT were not cytotoxic to the INS-1E cells (see Figures 1 and 2 in Chapter 3).

2.5 DOSE SELECTION

Although the non-occupational exposure levels for BNT(2,3D) and DBT are currently unknown, valuable environmental tissue data obtained midway through the project has aided in determining a concentration range that may be found in wildlife living in proximity to oil sands industrial activity in Northern Alberta. This tissue data was not available at the start of the project, and thus treatment doses used in the first set of experiments were based solely on the results obtained from the MTS assays.

Tissue concentrations of BNT(2,3D) and DBT in liver samples of otters retrieved from northern Alberta were generously provided by Dr. Philippe Thomas (Environment and Climate Change Canada). The average concentration of DBT in the otter samples was 163pM (range 20pM to 1.2 nM), while for BNT(2,3D) only a single measurement (39pM) was available. Therefore, the concentration range determined for DBT was also used for BNT(2,3D). Based on these data I chose to use the range of 10pM to 10nM for the S-HAC treatments in the functional assays described in this thesis.

2.6. QUANTITATIVE PCR

2.6.1 Experimental Protocol

Upon reaching 60% confluency INS-1E cells were treated with 1nM and 1μM BNT(2,3D) and DBT (N=5 independent experiments). Cells were treated for 48 hours after which the cells were harvested and RNA extracted using Trizol (ThermoFisher Scientific, Burlington, Ontario). Aliquots of media were also collected from each sample plate and stored at -80°C. RNA quality and quantity were assessed using the NanoDrop™ One microvolume spectrophotometer (Thermo Scientific, Burlington, Ontario). Contaminated RNA and/or samples with concentrations less than 500ng/μL were excluded from the study. Afterwards, RNA samples were standardized to 500ng/μL.

cDNA synthesis was performed on the RNA samples using the High Capacity cDNA Reverse Transcription Kit (ThermoFisher Scientific, Burlington, Ontario) following the kit protocol. Samples were run in the iCycler Thermal Cycler (Bio-Rad Laboratories, California, USA) with the following settings: 25°C for 10 minutes, 37°C for 2 hours and 85°C for 5 minutes. The generated cDNA product was stored at -20°C.

cDNA was diluted 1:40 in nuclease-free water. mRNA expression was measured by performing quantitative polymerase chain reactions (qPCR) using PerfeCTa SYBR Green fastmix (Quanta Biosciences, Massachusetts, USA). cDNA was plated in 384-well plate with sample size of n=5 per treatment group and control group, with triplicates per "n" sample. *Gapdh* and *18s* were used as housekeeping genes for both groups of treatments. Plates also contained NTC wells (in triplicate) as negative controls. PCR plates were then run in the CFX384 Touch™ Real-Time PCR Detection System (Bio-Rad Laboratories, California, USA) using one cycle of

polymerase activation (10 minutes at 95°C), 40 cycles of denaturation (15 seconds at 95°C) and 40 cycles of annealing/elongation (1 minute at 60°C).

In this project, qPCR experiments were run for the primary purpose of screening various target genes associated with glucose uptake, oxidative stress, ER stress, cell senescence and insulin production using the cDNA samples of INS-1E cells treated with 1nM and 1μM doses of BNT(2,3D) and DBT. Significant findings obtained from the screening process were used to determine key pathways altered by BNT(2,3D) and DBT which were then further examined using functional assays. For a detailed list of all examined target genes and their primer sequences, see Appendix 6.

2.6.2 Statistical Analysis

The CT values obtained for each treatment group and control group of each target gene were normalized to the geomean of the CT values obtained for the housekeeping genes *Gapdh* and *18s*. Fold change in gene expression was calculated for each sample of each target gene using the double delta Ct method (Livak & Schmittgen 2001). Outliers in the data were then detected and excluded using Grubbs test software (GraphPad, www.graphpad.com/quickcalcs/grubbs1). To detect statistically significant differences between treatment groups and control for each examined target gene, one-way ANOVA test is performed in SigmaPlot 11.0 software (Mahbobi & Tiemann 2015).

Prior to running one-way ANOVA, normality and equal variance tests are run for the data (Mahbobi & Tiemann 2015). Sample data that fails either test, is then run through the non-parametric Kruskal-Wallis test one-way ANOVA on ranks to detect statistically significant differences specifically between treatment groups and control (Mahbobi & Tiemann 2015).

Sample data that passes both the normality and equal variance tests, are then run through the parametric one-way ANOVA test (Mahbobi & Tiemann 2015). If a p-value below 0.05 was generated from the one-way ANOVA, post-hoc analysis, specifically the Holm-Sidak test, was performed in SigmaPlot 11.0 to identify the treatments group(s) which demonstrated statistically significant differences from the control group for each target gene (Silva-Veiga et al. 2018).

2.7. GLUCOSE UPTAKE

2.7.1 Experimental Protocol

A cell-based glucose uptake assay (Cayman Chemical, Michigan, USA) was run to measure the degree of glucose uptake in beta cells. INS-1E cells were seeded in black, clear bottom 96-well plates at a seeding density of 150,000 cells/ml for 24 hours. Afterwards, INS-1E cells were treated in duplicate for 44 hours with glucose-containing media containing 1pM, 10pM, 100pM, 1nM, 10nM, 100nM and 1μM doses (N=5 independent experiments). After 44 hours, treated media was removed and replaced with glucose-free RPMI 1640 media supplemented with 2mM L-glutamine (Corning, Virginia, USA) as well as 50uM 2-mercaptoethanol, 10% heat-inactivated fetal bovine serum (Hyclone, Utah, USA), 1mM sodium pyruvate (GIBCO, Burlington, Ontario), 1% penicillin and streptomycin (GIBCO, Burlington, Ontario) that contains BNT(2,3D) and DBT at the same doses for 2 hours. After 2 hours, the fluorescently tagged glucose analog 2-NBDG was added to each well to a final concentration of 100μg/mL. After a 2-hour incubation with 2-NBDG, fluorescence was read at excitation/emission of 485/535 nm respectively in the Synergy H4 Hybrid microplate reader (BioTek Instruments, Vermont, USA).

2.7.2 Statistical Analysis

Outliers in the data were then detected and excluded using online Grubbs test software (GraphPad, www.graphpad.com/quickcalcs/grubbs1). Normality and equal variance tests were run for the data (Mahbobi & Tiemann 2015). Data passed both tests and one-way ANOVA test was performed in SigmaPlot 11.0 software to detect statistically significant differences between treatment groups and control group (Mahbobi & Tiemann 2015). If a p-value below 0.05 was generated from the one-way ANOVA, post-hoc analysis, specifically the Holm-Sidak test, was performed in SigmaPlot 11.0 to identify the treatments group(s) which demonstrated statistically significant differences from the control group (Silva-Veiga et al. 2018).

2.8. INTRACELLULAR ROS

2.8.1 Experimental Protocol

To determine if S-HACs can induce ROS accumulation, intracellular ROS concentrations were measured in the beta cells treated with the selected S-HACs. INS-1E cells were seeded in a 96-well plate at seeding density of 175,000 cells/mL for 24 hours after which the fluorescent intracellular ROS assay with DCFH-DA (Cell Biolabs, California, USA) was run according to the manufacturer's instructions. Upon incubation of INS-1E cells for 1 hour with DCFH-DA, cells were washed and afterwards treated with BNT(2,3D) and DBT at 1nM and 1μM doses in duplicate (N=5 independent experiments) for 1 hour. After 1 hour, fluorescence was read at excitation/emission of 480/530 nm respectively in the Synergy H4 Hybrid microplate reader (BioTek Instruments, Vermont, USA).

2.8.2 Statistical Analysis

Outliers in all data sets were detected and excluded using online Grubbs test software (GraphPad, www.graphpad.com/quickcalcs/grubbs1). Equal variance and normality tests were performed, however data failed normality test. Consequently, the non-parametric ANOVA on ranks test was performed on SigmaPlot 11.0 to detect statistically significant differences between treatment groups and control group for each treatment compound. Afterwards, post-hoc analysis, specifically the pairwise multiple comparisons Tukey test, was performed in SigmaPlot 11.0 (Brown 2005). The treatments group(s) which demonstrated statistically significant differences from the control group were identified.

2.9. CELL SENESCENCE

2.9.1 Experimental Protocol

To determine if S-HACs can induce cell senescence in beta cells, a senescence histochemical staining assay (Sigma, St. Louis, Missouri, USA) was run. INS-1E cells were cultured in 6-well plates and then treated for 48 hours with 10pM, 100pM, 1nM and 10nM doses of BNT(2,3D) and DBT (N=3 independent experiments). Following a 48-hour incubation, cells were fixed and stained with X-gal solution and incubated overnight at 37°C. The degree of cellular senescence in treated plates was determined by manual cell counting and calculating the percentage of senescent cells (i.e. β-gal positive cells) in each well relative to the total number of cells using the AE2000 inverted microscope (Motic, Kowloon Bay, Hong Kong).

2.9.2 Statistical Analysis

Outliers in the data were then detected and excluded using online Grubbs test software (GraphPad, www.graphpad.com/quickcalcs/grubbs1). Normality and equal variance tests were

run for the data (Mahbobi & Tiemann 2015). Data passed both tests and one-way ANOVA test was performed in SigmaPlot 11.0 software to detect statistically significant differences between treatment groups and control group (Mahbobi & Tiemann 2015). If a p-value below 0.05 was generated from the one-way ANOVA, post-hoc analysis, specifically the Holm-Sidak test, was performed in SigmaPlot 11.0 to identify the treatments group(s) which demonstrated statistically significant differences from the control group (Silva-Veiga et al. 2018).

2.10. INTRACELLULAR INSULIN PRODUCTION

2.10.1 Experimental Protocol

To determine the effects of BNT(2,3D) and DBT on insulin production, an ultrasensitive rat insulin ELISA (Crystal Chem, Illinois, USA) was run using protein extracted from INS-1E cells treated with BNT(2,3D) and DBT.

INS-1E cells were cultured in 10cm dishes and upon reaching 60% confluency were treated for 48 hours with BNT(2,3D) and DBT at 1pM, 10pM, 100pM, 1nM, 10nM and 1μM doses (N=5 independent experiments). After 48 hours of treatment, the treated cells were harvested with RIPA lysis buffer containing 1% of Triton X-100, 0.1% of sodium dodecyl sulfate, 150mM of NaCl, 50mM of Tris-HCl (at a pH of 8.0), 0.5% of sodium deoxycholate and complete mini EDTA-free protease inhibitor cocktail tablets (Roche, Laval, Quebec). The lysate was then sonicated for 15-20 seconds and centrifuged at 13,000 rpm for 15 minutes at 4°C. The supernatant was collected and stored in aliquots at -80°C.

Quantification of total insulin content in sample vial was determined by normalizing insulin content to total protein content. Thus, total protein in each sample was quantified using Pierce BCA protein assay kit (ThermoFisher Scientific, Burlington, Ontario) following manufacturer's

instructions. Albumin standards were prepared using RIPA buffer as the diluent. The standard curve and absorbance values obtained for each sample from BCA assay were used to interpolate total protein content using 4 parameter-logistic regression (4PL), for greater accuracy. Total protein content in all samples (μg/mL) were in the higher end of the standard curve. Thus, samples were diluted 500-fold (1:500), with DPBS as the diluent, prior to plating samples in insulin ELISA.

The ultrasensitive rat insulin ELISA (Crystal Chem, Illinois, USA) was conducted according to the manufacturer's instructions using the diluted (1:500) protein samples. Absorbance was read at 450nm and 630nm in the Synergy H4 Hybrid microplate reader (BioTek Instruments, Vermont, USA). Prior to further analysis, absorbance values at 630nm were subtracted from absorbance values at 450nm. Insulin content was then interpolated using 4PL. Insulin content (in ng/mL) and total protein content (in μg/mL) were then multiplied by total volume in sample vial (in mL) to determine total mass of insulin (in ng) and total mass of protein (in μg). Total insulin per sample was then normalized to total protein per sample (unit of ng/μg).

2.10.2 Statistical Analysis

Outliers in the data were then detected and excluded using online Grubbs test software (GraphPad, www.graphpad.com/quickcalcs/grubbs1). Normality and equal variance tests were run for the data (Mahbobi & Tiemann 2015). Data passed both tests and one-way ANOVA test was performed in SigmaPlot 11.0 software to detect statistically significant differences between treatment groups and control group (Mahbobi & Tiemann 2015). If a p-value below 0.05 was generated from the one-way ANOVA, post-hoc analysis, specifically the Holm-Sidak test, was performed in SigmaPlot 11.0 to identify the treatments group(s) which demonstrated statistically significant differences from the control group (Silva-Veiga et al. 2018).

CHAPTER 3 – RESULTS

3.1 Cytotoxicity of Compounds

BNT(2,3D) and DBT at doses up to 10μM did not cause cytotoxicity in INS-1E cells after 48 hours of treatment (Figures 1 and 2).

3.2 Glucose Uptake

The mRNA expression of *Glut2*, encoding the glucose transporter GLUT2, was measured in INS-1E cells treated with BNT(2,3D) and DBT for 48 hours. Steady-state mRNA expression of *Glut2* was significantly upregulated by both BNT(2,3D) and DBT at all doses examined (Figure 3). Subsequently, a glucose uptake assay was run in which uptake of the fluorescently tagged glucose analog 2-NBDG was measured in INS-1E cells treated with BNT(2,3D) and DBT for 48 hours. In the glucose uptake assay, BNT(2,3D) significantly increased the uptake of 2-NBDG at 1pM in the INS-1E cells, while DBT significantly increased 2-NBDG uptake at the 1pM, 1nM, 100nM and 1μM doses (Figure 4). In addition, the mRNA expression of the glycolytic gene *Gck* was measured in INS-1E cells treated with BNT(2,3D) and DBT for 48 hours. BNT(2,3D) upregulated mRNA expression of *Gck* at 1nM, however mRNA expression of *Gck* was not altered by DBT at either dose (Figure 5). Statistically significant differences detected between treatment groups and control generated a p-value less than 0.05.

3.3 ROS Production

The mRNA expression of antioxidant-associated genes *Nrf2*, *Sod2*, *Catalase* and *Gpx* were measured in INS-1E cells treated with BNT(2,3D) and DBT for 48 hours. Both BNT(2,3D) and DBT significantly upregulated the mRNA expression of *Nrf2*, *Sod2* and *Catalase* in the INS-1E cells (Figure 6). *Nrf2* expression was significantly upregulated by BNT(2,3D) at 1μM and by

DBT at both doses examined (Figure 6A). *Sod2* expression was significantly upregulated by both S-HACs at all examined doses in a dose-dependent manner (Figure 6B). *Catalase* expression was significantly upregulated by BNT(2,3D) at 1nM and by DBT at both doses examined (Figure 6C). The mRNA expression of *Gpx* was not altered by either S-HAC. Subsequently, a fluorescent ROS assay was run to measure intracellular ROS levels in INS-1E cells treated with BNT(2,3D) and DBT for 1 hour. Both S-HACs significantly increased ROS production in INS-1Es at the 1nM dose; no effect was observed at the 1μM dose (Figure 7). In addition, mRNA expression of the oxidative damage-responsive gene *p53* was also measured, however neither S-HAC altered its expression (Figure 8). Statistically significant differences detected between treatment groups and control generated a p-value less than 0.05.

3.4 Cell Senescence

The mRNA expression of the senescence-inducing gene *p21,* SA-β Gal encoding gene *Glb1* and anti-apoptotic gene *Bcl2* were measured in INS-1E cells treated with BNT(2,3D) and DBT for 48 hours. *p21* expression was significantly upregulated by BNT(2,3D) at the 1μM dose but was not altered by DBT at either dose (Figure 9). However, there was a significant upregulation of the other senescence markers *Glb1* and *Bcl2* by both BNT(2,3D) and DBT at all doses examined (Figure 10). Subsequently, a senescence histochemical staining assay was run to measure the degree of cellular senescence in INS-1E cells treated with BNT(2,3D) and DBT for 48 hours. BNT(2,3D), but not DBT, significantly induced cellular senescence in INS-1E cells at the 10pM, 100pM and 1nM doses (Figure 11). All statistically significant differences detected between treatment groups and control generated a p-value less than 0.05.

3.5 Senescence-Associated Secretory Phenotype

Following the observed increase in cellular senescence in INS-1E sample populations, mRNA expression of the pro-inflammatory SASP markers *Nlrp3*, *Il1b*, *Serpine1*, *Mcp1* and *Il6* were measured in INS-1E cells treated with BNT(2,3D) and DBT for 48 hours. Expression of *Nlrp3*, which regulates IL1β protein activity (Barnes 2015), was significantly upregulated by DBT at 1nM, however, *Il1b* expression was not upregulated by either S-HAC (Figure 12A and 12B). *Serpine1* expression was significantly upregulated by BNT(2,3D) at all examined doses and by DBT at 1nM (Figure 12C). *Mcp1* expression was significantly upregulated by DBT at 1nM, but was not altered by BNT(2,3D) at either dose (Figure 12D). Lastly, *Il6* expression was significantly upregulated by DBT at 1nM, but was not upregulated by BNT(2,3D) at either dose (Figure 12E). Statistically significant differences detected between treatment groups and control generated a p-value less than 0.05.

3.6 ER Stress

The mRNA expression of ER stress markers *Atf6, Grp78, Txnip* and *Chop* were measured in INS-1E cells treated with BNT(2,3D) and DBT for 48 hours. *Atf6* expression was significantly upregulated by BNT(2,3D) at 1μM and by DBT at 1nM (Figure 13A). *Grp78* expression was significantly upregulated by DBT at 1nM but was not altered by BNT(2,3D) at either dose (Figure 13B). *Txnip* and *Chop* expression were significantly upregulated by BNT(2,3D) at 1μM, but were unaltered by DBT (Figure 13C and Figure 13D). Statistically significant differences detected between treatment groups and control generated a p-value less than 0.05.

3.7 Insulin Production

The mRNA expression of *Pdx1*, *Mafa*, *Isl1* and *Ins2*, markers associated with insulin production, were measured in INS-1E cells treated with BNT(2,3D) and DBT for 48 hours. *Pdx1* expression was significantly upregulated by BNT(2,3D) at 1μM, but was unaltered by DBT at either dose (Figure 14A). The mRNA expression of *Mafa* was not altered by either S-HAC (Figure 14B). *Isl1* expression was significantly upregulated by BNT(2,3D) at 1nM and by DBT at all examined doses (Figure 14C). *Ins2* expression was significantly upregulated by BNT(2,3D) at 1μM but was unaltered by DBT at either dose (Figure 14D). Subsequently, an insulin ELISA was run to measure insulin content in INS-1E cells treated with BNT(2,3D) and DBT for 48 hours. DBT significantly increased insulin production at the 10nM dose in INS-1E cells, however no changes to intracellular insulin content were observed in INS-1E cells treated with BNT(2,3D) at any of the examined doses (Figure 15). All statistically significant differences detected between treatment groups and control generated a p-value less than 0.05.

3.8 Insulin Secretion

The mRNA expression of *Kcnj11*, which encodes for a component in the K_{ATP} channel and is associated with insulin secretion, was measured in INS-1E cells treated with BNT(2,3D) and DBT for 48 hours. *Kcnj11* expression was significantly upregulated by BNT(2,3D) at 1μM dose ($p<0.05$) but was unaltered by DBT at either dose (Figure 16).

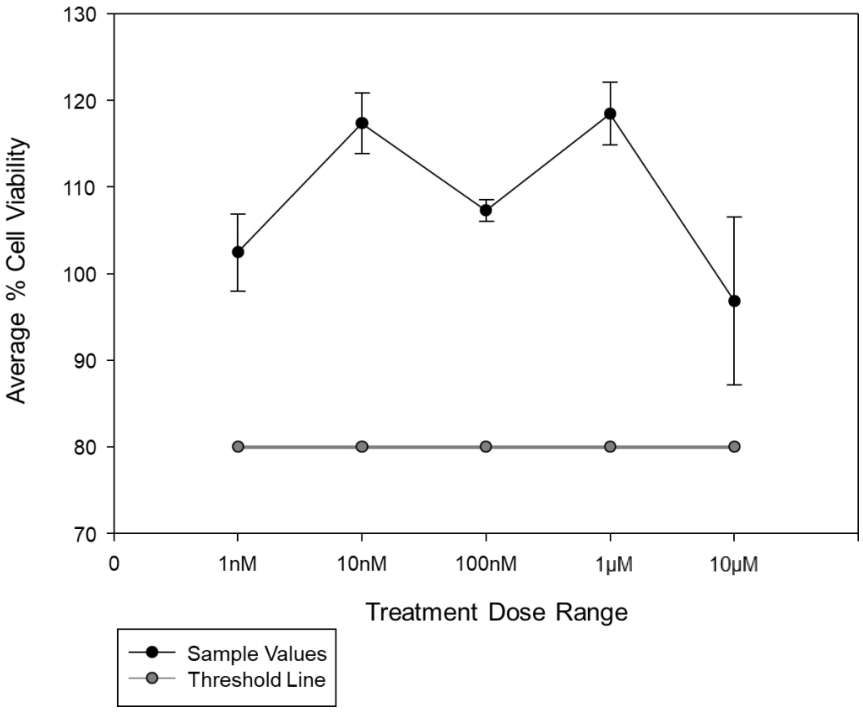

Figure 1. Percent cell viability of INS-1E cells treated with BNT(2,3D) at 1nM, 10nM, 100nM, 1µM and 10µM doses for 48 hours (n=5). 80% cell viability threshold line shown as straight dashed line.

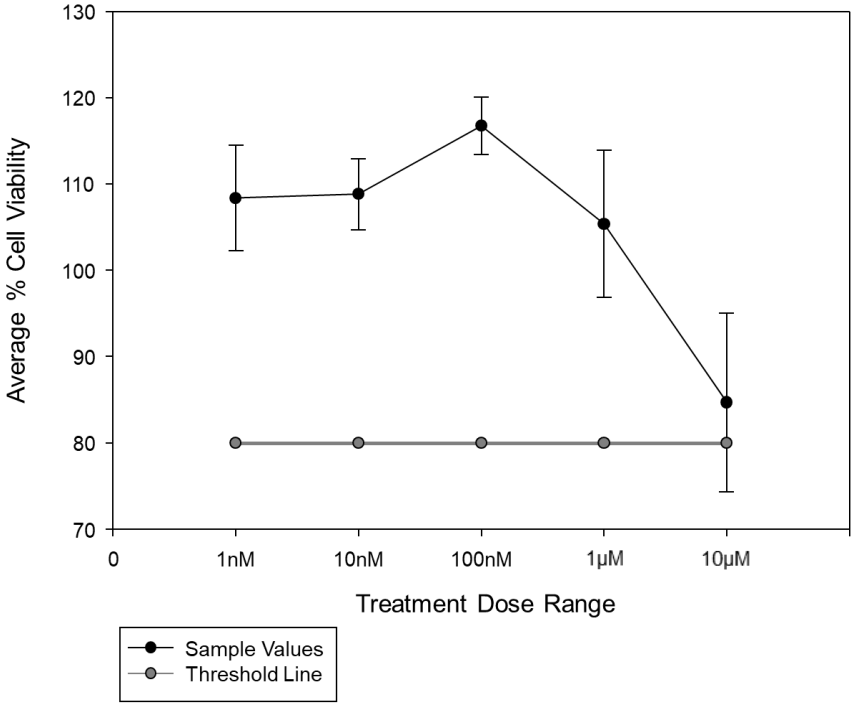

Figure 2. Percent cell viability of INS-1E cells treated with DBT at 1nM, 10nM, 100nM, 1µM and 10µM doses for 48 hours (n=5). 80% cell viability threshold line shown as straight dashed line.

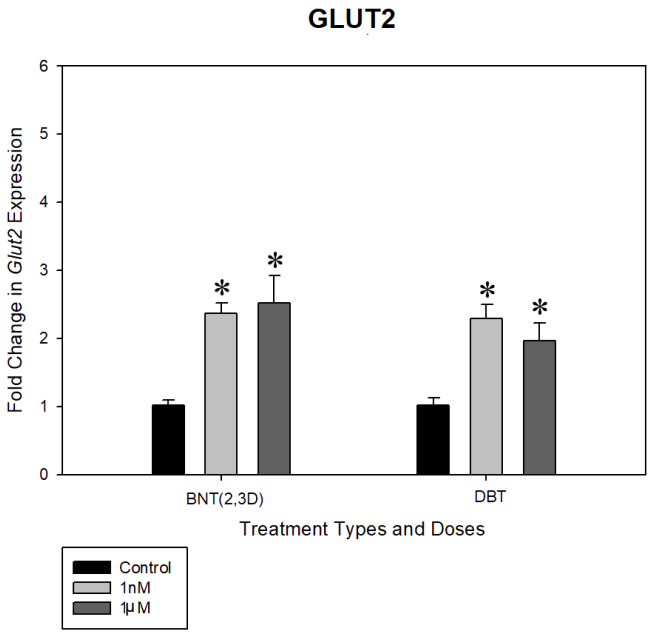

Figure 3. mRNA expression of glucose transporter gene *Glut2* in INS-1E cells treated with BNT(2,3D) and DBT at 1nM and 1µM doses for 48 hours (n=5). Data presented as mean ± SEM. Bars with an asterisk are statistically different from their respective control group ($p < 0.05$).

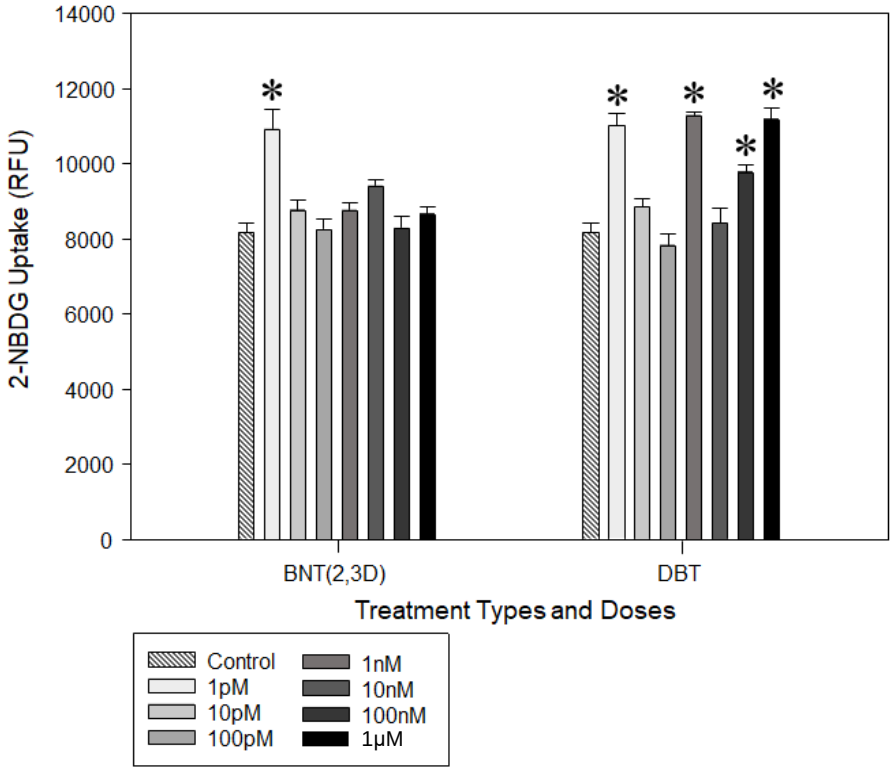

Figure 4. Fluorescence readings for glucose uptake in INS-1E cells treated with BNT(2,3D) and DBT at 1pM, 10pM, 100pM, 1nM, 10nM, 100nM and 1µM doses for 48 hours (n=5). Data presented as mean ± SEM. Bars with an asterisk are statistically different from their respective control group ($p < 0.05$).

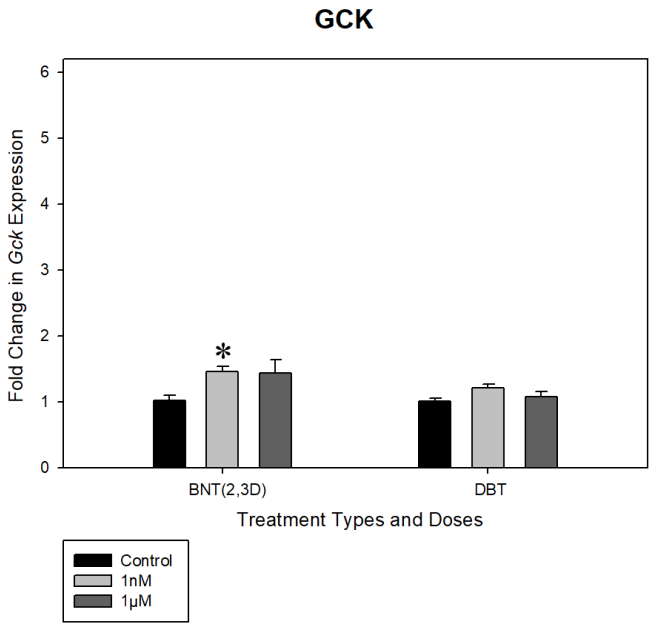

Figure 5. mRNA expression of glycolytic gene *Gck* in INS-1E cells treated with BNT(2,3D) and DBT at 1nM and 1μM doses for 48 hours (n=5). Data presented as mean ± SEM. Bars with an asterisk are statistically different from their respective control group ($p<0.05$).

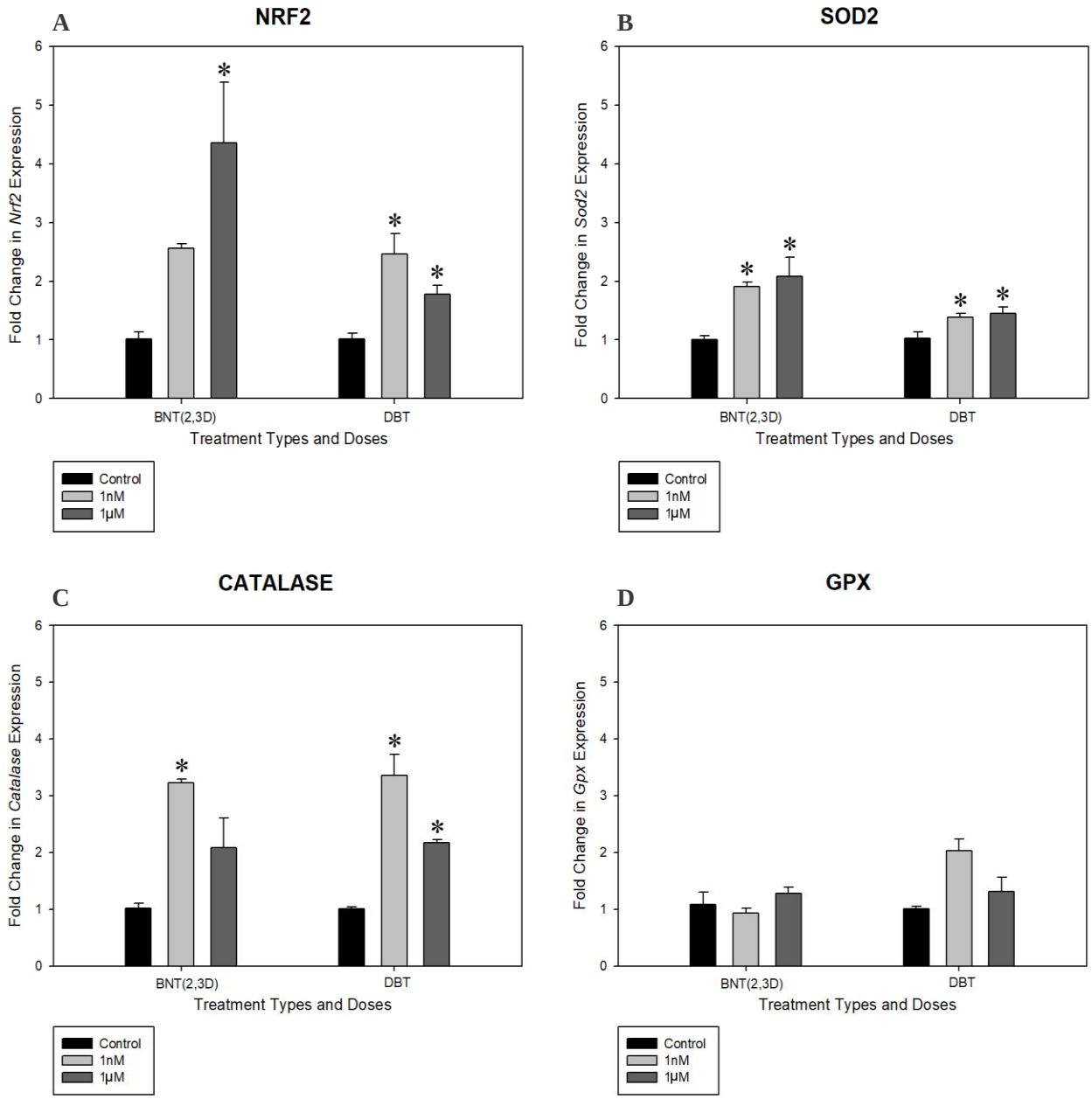

Figure 6. mRNA expression of *Nrf2* (**A**), *Sod2* (**B**), *Catalase* (**C**) and *Gpx* (**D**); target genes associated with antioxidant expression in INS-1E cells treated with BNT(2,3D) and DBT at 1nM and 1μM doses for 48 hours. Data presented as mean ± SEM. Bars with an asterisk are statistically different from their respective control group.

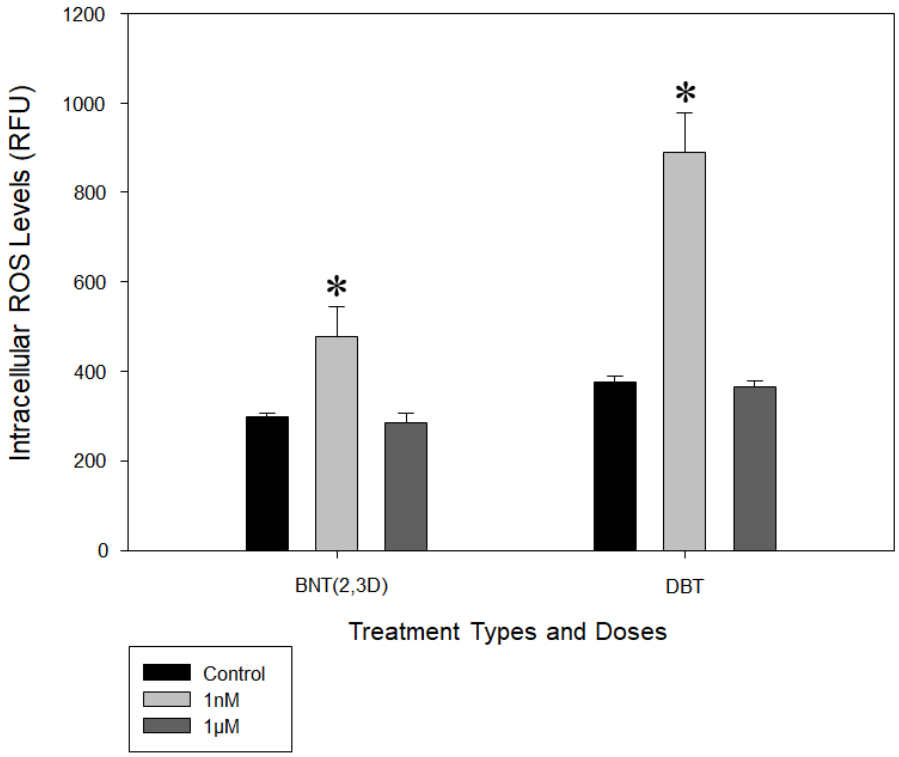

Figure 7. Fluorescence readings for ROS measurement in INS-1E cells treated with BNT(2,3D) and DBT at at 1nM and 1µM doses for 1 hour (n=5). Data presented as mean ± SEM. Bars with an asterisk are statistically different from their respective control group ($p < 0.05$).

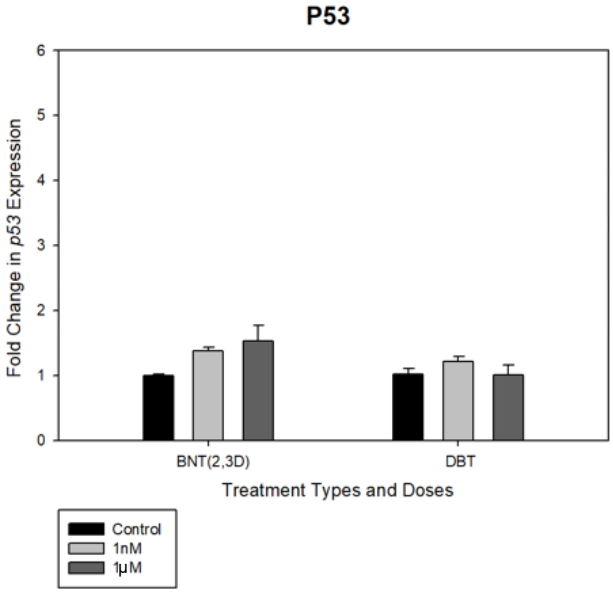

Figure 8. mRNA expression of *p53* in INS-1E cells treated with BNT(2,3D) and DBT at 1nM and 1µM doses for 48 hours (n=5). Data presented as mean ± SEM. Bars with an asterisk are statistically different from their respective control group ($p < 0.05$).

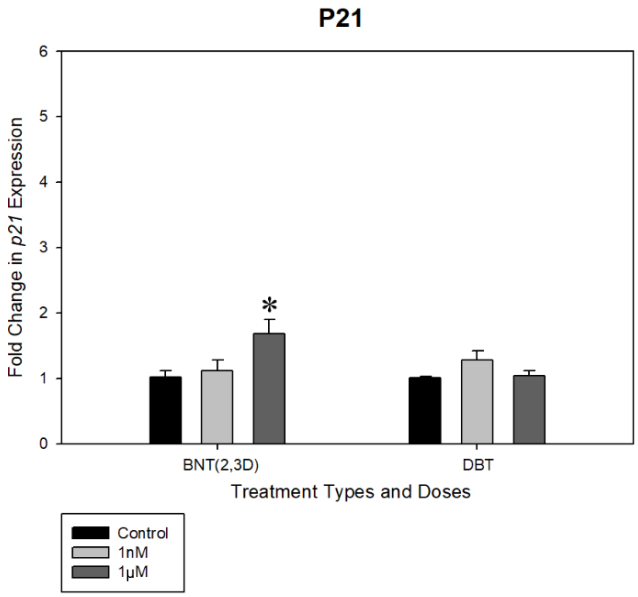

Figure 9. mRNA expression of *p21* in INS-1E cells treated with BNT(2,3D) and DBT at 1nM and 1μM doses for 48 hours (n=5). Data presented as mean ± SEM. Bars with an asterisk are statistically different from their respective control group ($p < 0.05$).

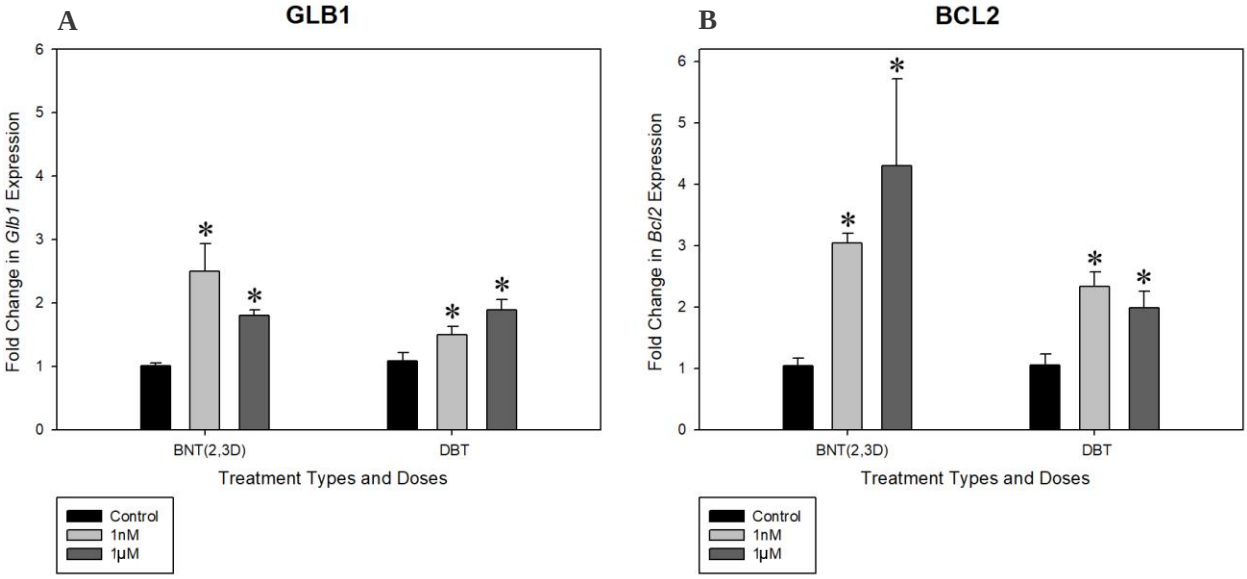

Figure 10. mRNA expression of *Glb1* (**A**) and *Bcl2* (**B**), target genes associated with cell senescence in INS-1E cells treated with BNT(2,3D) and DBT at 1nM and 1μM doses for 48 hours (n=5). Data presented as mean ± SEM. Bars with an asterisk are statistically different from their respective control group ($p < 0.05$).

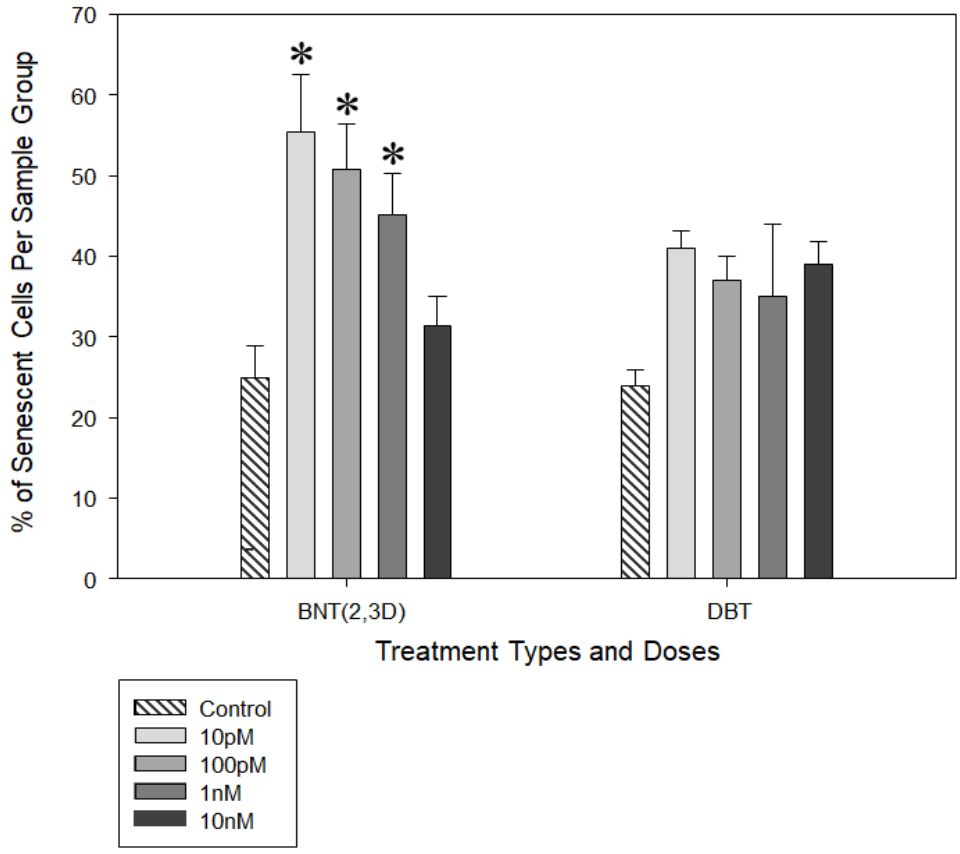

Figure 11. Percentage of senescent INS-1E cells in sample plates treated with BNT(2,3D) and DBT at 10pM, 100pM, 1nM and 10nM doses for 48 hours (n=3). Data presented as mean ± SEM. Bars with an asterisk are statistically different from their respective control group ($p < 0.05$).

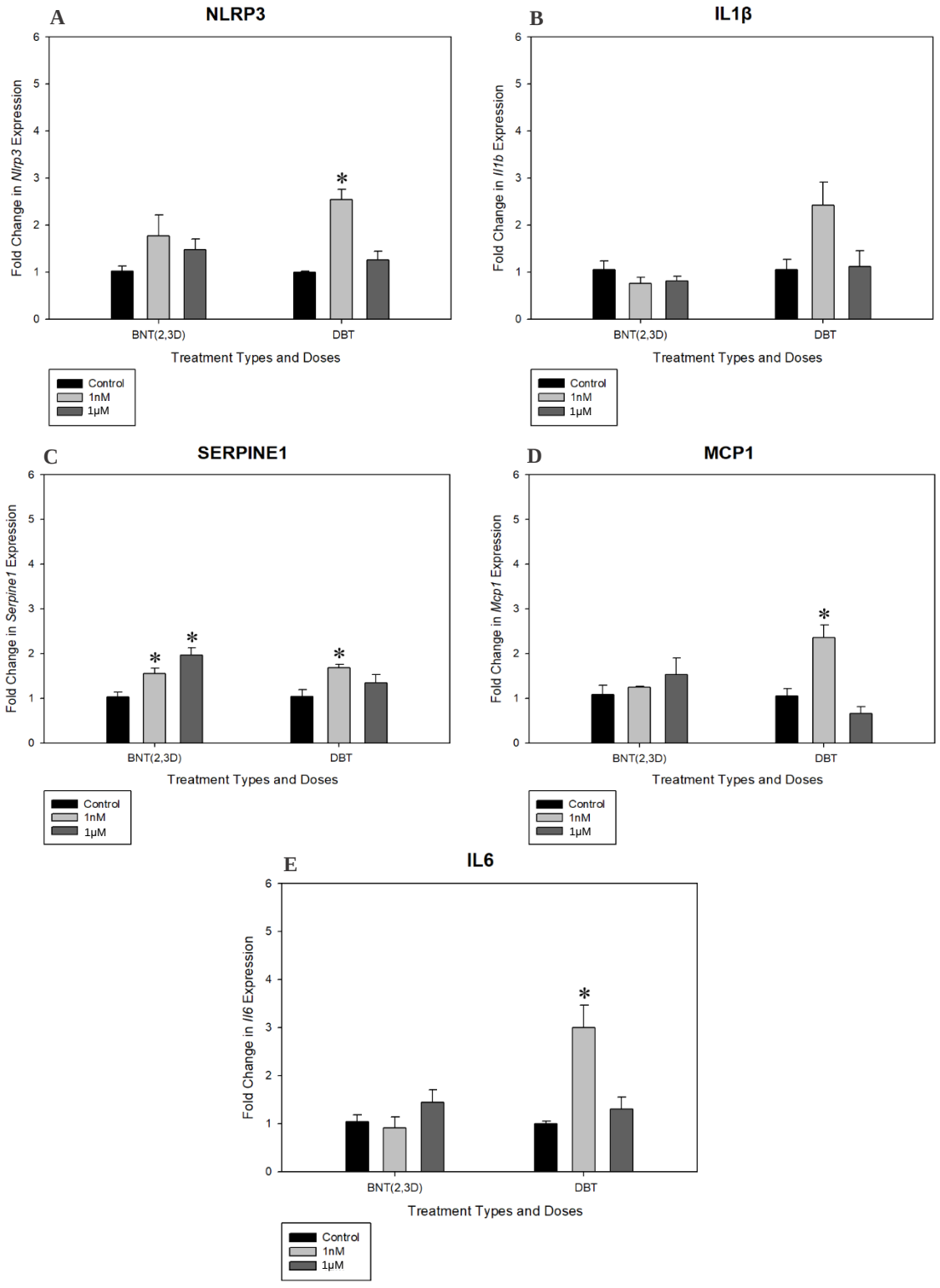

Figure 12. mRNA expression of *Nlrp3* (**A**), *Il1b* (**B**), *Serpine1* (**C**), *Mcp1* (**D**) and *Il6* (**E**); target genes associated with SASP in INS-1E cells treated with BNT(2,3D) and DBT at 1nM and 1μM doses for 48 hours (n=5). Data presented as mean ± SEM. Bars with an asterisk are statistically different from their respective control group ($p < 0.05$).

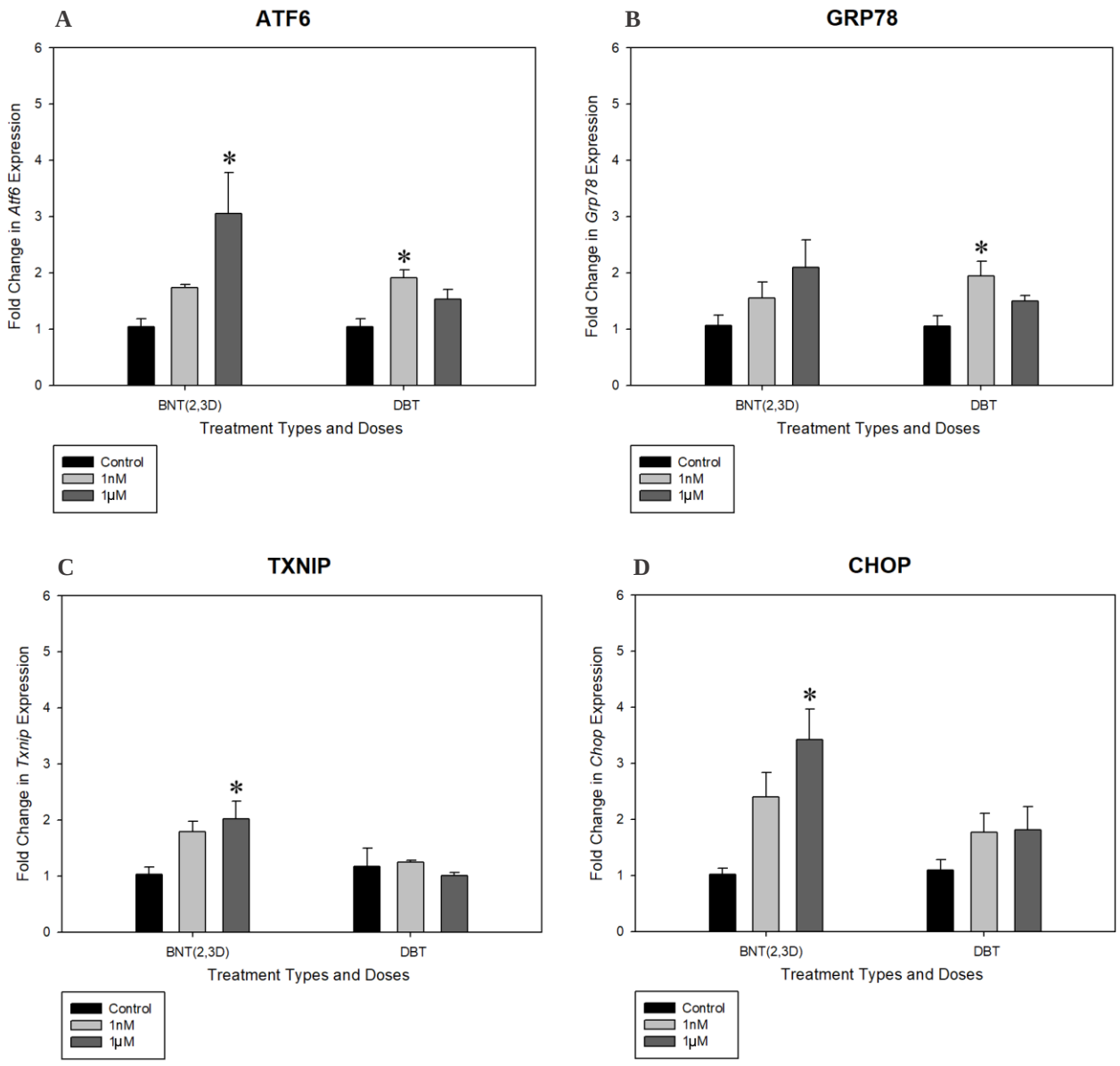

Figure 13. mRNA expression of *Atf6* (**A**), *Grp78* (**B**), *Txnip* (**C**) and *Chop* (**D**); target genes associated with ER stress in INS-1E cells treated with BNT(2,3D) and DBT at 1nM and 1μM doses for 48 hours (n=5). Data presented as mean ± SEM. Bars with an asterisk are statistically different from their respective control group ($p < 0.05$).

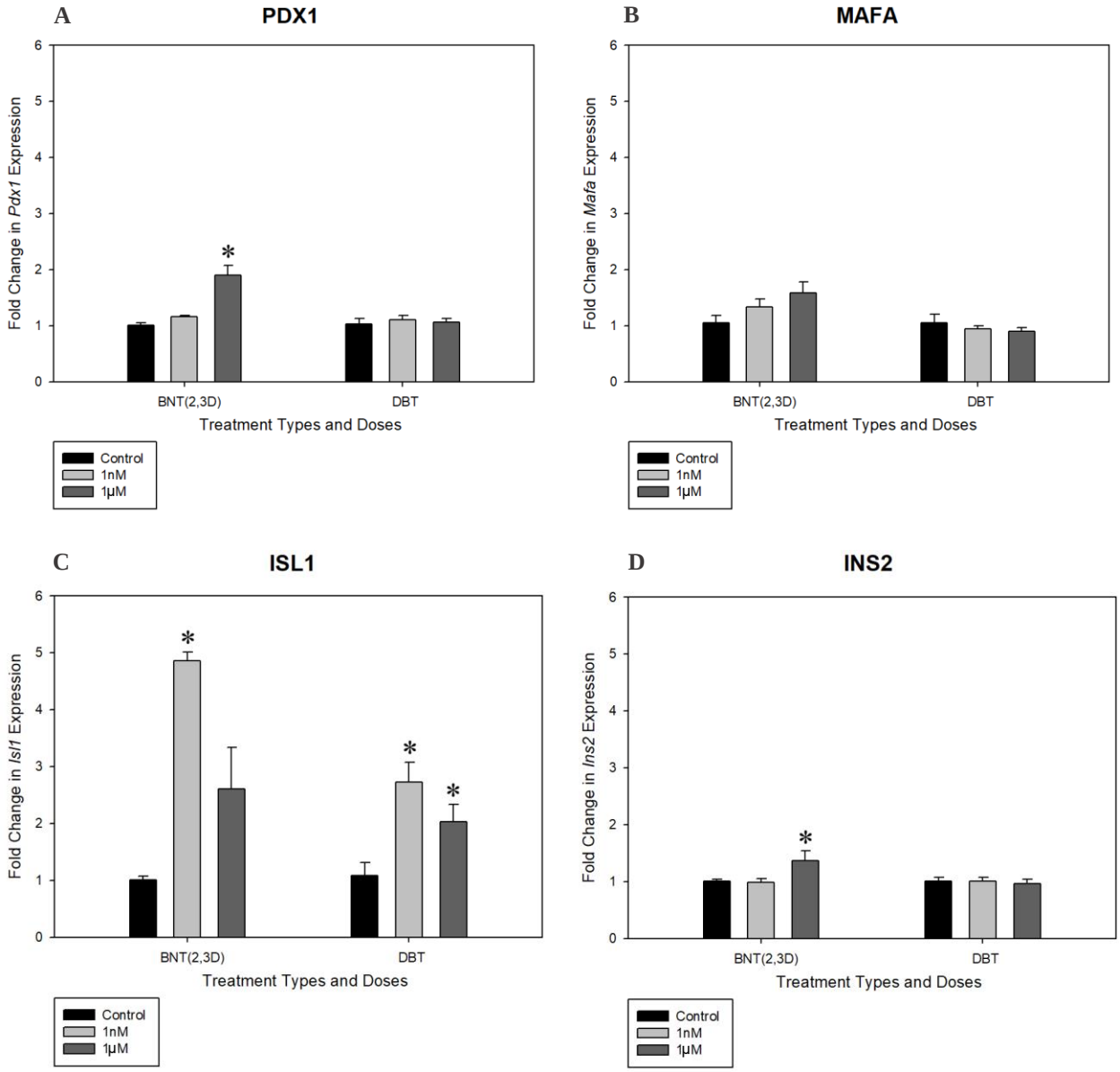

Figure 14. mRNA expression of *Pdx1* (**A**), *Mafa* (**B**), *Isl1* (**C**) and *Ins2* (**D**); target genes associated with insulin production and secretion in INS-1E cells treated with BNT(2,3D) and DBT at 1nM and 1μM doses for 48 hours (n=5). Data presented as mean ± SEM. Bars with an asterisk are statistically different from their respective control group ($p < 0.05$).

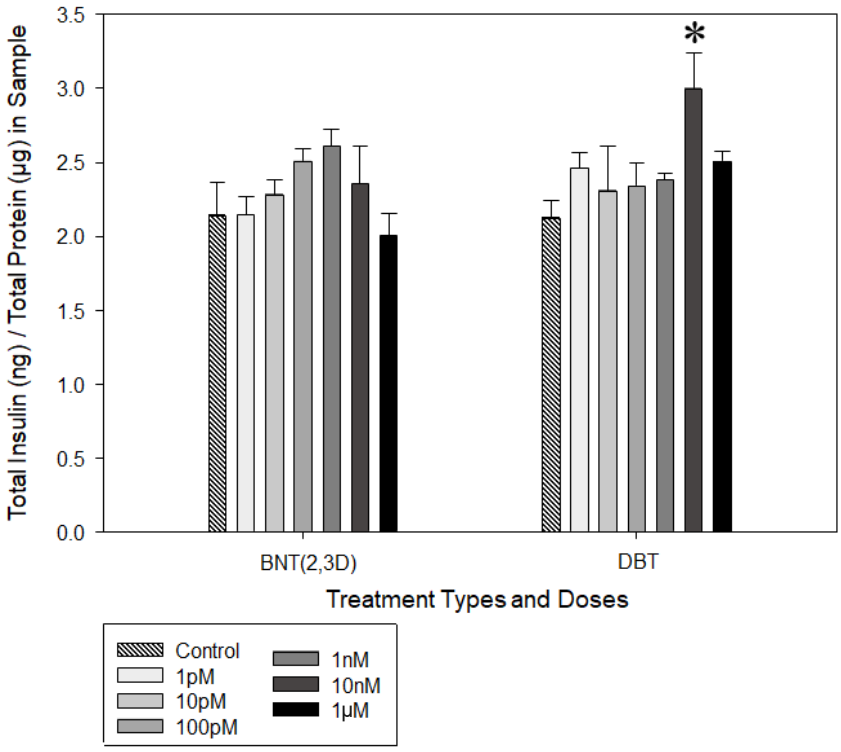

Figure 15. Ratio of total insulin content to total protein in INS-1E cells treated with BNT(2,3D) and DBT at 1pM, 10pM, 100pM, 1nM, 10nM and 1µM doses for 48 hours (n=5). Data presented as mean ± SEM. Bars with an asterisk are statistically different from their respective control group ($p < 0.05$).

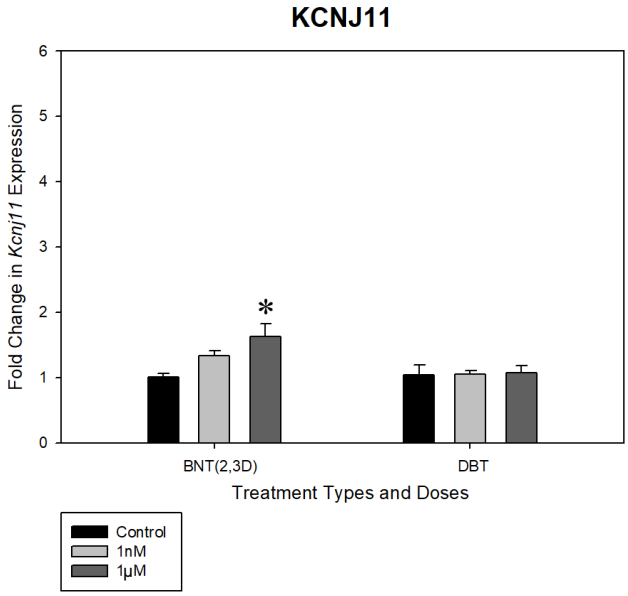

Figure 16. mRNA expression of *Kcnj11* in INS-1E cells treated with BNT(2,3D) and DBT at 1nM and 1µM doses for 48 hours (n=5). Data presented as mean ± SEM. Bars with an asterisk are statistically different from their respective control group ($p < 0.05$).

CHAPTER 4 – DISCUSSION

The results generated in this thesis have identified a number of potential pathways through which S-HACs may affect pancreatic beta cell health and function. First, S-HAC exposure increases intracellular ROS production in beta cells. S-HAC exposure may also be associated with increased glucose uptake and metabolism in the beta cells. S-HAC exposure may also induce ER stress in the beta cells, likely through ROS accumulation. ROS buildup may also induce cell senescence, potentially through a P53-independent pathway. The senescent beta cells remain metabolically active and continue to produce relatively the same quantity of insulin as non-senescent beta cells; however, the rate at which the insulin is secreted from the senescent cells may differ.

4.1 S-HACs and Glucose Uptake

Glucose uptake was increased in beta cells treated with BNT(2,3D) and DBT at concentrations within the range that has been reported in wildlife samples. Upregulation in mRNA expression of *Gck* by BNT(2,3D) was also observed, suggesting increased metabolism of the consumed glucose. Increased glucose uptake is one of the primary inducers of various cellular stresses in the beta cell including ROS accumulation and ER stress (Hasnain et al. 2016). Interestingly, increased glucose uptake, increased ROS production and increased mRNA expression of ER stress markers was observed in the beta cells exposed to 1nM of DBT. This suggests the plausibility that non-occupational exposures of these S-HACs, particularly DBT, that could have an impact on glucose uptake, that in turn may induce cellular stress in the exposed beta cell.

However, it is unclear the molecular mechanism(s) through which BNT(2,3D) and DBT may contribute to increasing glucose uptake in exposed beta cells. One potential mechanism may be through interacting with insulin receptors in the beta cell membrane by functioning as an insulin receptor ligand. PACs, the broader class of aromatic compounds to which S-HACs belong to, have been shown to be associated with regulating the expression of a major downstream target of the insulin receptor in the beta cell, insulin receptor substrate 2 (Kim et al. 2016). The potential for PACs to interact with insulin receptors on beta cells suggests that S-HACs may also possess this same binding capacity.

Furthermore, insulin receptors have been demonstrated to play a role in regulating glucose uptake by regulating the mRNA expression of *Glut2* (Wang et al. 2018). The mRNA expression of *Glut2*, which encodes the glucose receptor present in beta cells, was significantly upregulated by both BNT(2,3D) and DBT at all examined doses. This suggests therefore that both S-HACs may be interacting with insulin receptors on the beta cell membrane to alter *Glut2* expression and upregulate glucose uptake.

4.2 S-HACs Increase ROS Production

Both BNT(2,3D) and DBT significantly increase the production of ROS in exposed beta cells. ROS accumulation upregulates the mRNA expression of the ROS-responsive transcription factor *Nrf2* and consequently upregulates the mRNA expression of important antioxidant genes *Sod2* and *Catalase*. Neither S-HAC altered the mRNA expression of *Gpx*. In mammalian cells, the GPX enzyme has a higher affinity for the ROS H_2O_2 than the CATALASE enzyme (Baud et al. 2004). Thus, CATALASE is required at a much higher concentration to elicit detoxifying effects of the same magnitude as GPX (Baud et al. 2004). However, it is important to note that

while mRNA expression of a target gene is a strong indicator of protein expression, increased mRNA expression does not always equate to increased protein expression (Edfors et al. 2016). Therefore, although mRNA expression of antioxidant genes was upregulated, it is unknown whether protein expression of these antioxidants was also upregulated. Furthermore, pancreatic islets produce smaller quantities of the NRF2 targets SOD2, GPX, and CATALASE than most tissues in the body, demonstrating the weak antioxidant capacity of pancreatic beta cells (Miki et al. 2018). Therefore, S-HACs may be generating ROS in the mitochondria at a rate too high to be compensated by an increase in antioxidant expression by the beta cell, thereby leading to ROS accumulation (Miki et al. 2018).

ROS accumulation, in response to S-HAC exposure, was also observed in a study examining DBT-treated human neuroblastoma cells (Sarma et al. 2017). This study has also shown that in addition to increasing ROS production, DBT also lowered the mitochondrial membrane potential of the DBT-treated neuroblastoma cells (Sarma et al. 2017). Mitochondrial membrane potential is an important indicator of mitochondrial function (Zorova et al. 2018). It is suggested that the accumulation of ROS by DBT may impair mitochondrial function in the exposed cells (Sarma et al. 2017). Furthermore, DBT exposure also induced oxidative stress in the neuroblastoma cells and upregulated the expression of oxidative stress-responsive proteins (Sarma et al. 2017). Therefore, it is plausible that the accumulation of ROS in beta cells exposed to DBT and BNT(2,3D) may lead to the development of oxidative stress and the impairment of important cellular functions in these beta cells, including mitochondrial activity.

4.3 S-HACs May Induce ER Stress

S-HACs upregulated the gene expression of *Atf6*, *Grp78*, *Txnip* and *Chop*, components of the unfolded protein response, suggesting that these S-HACs may induce ER stress in the beta cells. The ER stress may be induced due to increased glucose uptake and increased ROS production in the S-HAC exposed beta cells. Increased glucose uptake and metabolism has been shown to increase insulin biosynthesis and the accumulation of misfolded and unfolded proteins, leading to ER stress (Burgos-Moron et al. 2019; Eizirik et al. 2007). However, insulin content in beta cells exposed to the S-HACs was not significantly different from the control group, even at doses where glucose uptake was increased in the exposed beta cells. Furthermore, the doses at which mRNA expression of the ER stress markers were upregulated in the beta cells exposed to BNT(2,3D) did not reflect the doses at which glucose uptake was increased. Similarly, DBT overall did not display a relationship between increased glucose uptake and increased mRNA expression of ER stress markers. Therefore, the observed increase in mRNA expression of ER stress markers by the selected S-HACs may be not be due to increased glucose uptake.

Alternatively, increased ER stress may be due to the accumulation of intracellular ROS, particularly H_2O_2. H_2O_2 has been shown to activate the 3 main pathways of the UPR through phosphorylation or proteolytic cleavage of the ER stress sensor proteins: IRE1, PERK and ATF6 (Pallepati & Averill-Bates 2011). H_2O_2 has also been shown to upregulate the expression of the ER chaperone GRP78 (Pallepati & Averill-Bates 2011). Both *Grp78* and *Atf6* were upregulated in INS-1E cells exposed to DBT at 1nM dose; the same dose which caused a significant upregulation of ROS production. However, neither *Chop* nor *Txnip* were upregulated following exposure to 1nM of DBT. Increased expression of GRP78 and ATF6 by DBT can increase protein folding in the beta cell (Ye et al. 2018). Increased protein folding generates large

quantities of H_2O_2 which diffuses freely across many compartments in the cell, including the mitochondria and ER (Pluquet et al. 2014). This creates a vicious cycle that sustains ER stress conditions and further increases intracellular ROS concentrations (Burgos-Moron et al. 2019).

ER stress may be induced in beta cells by BNT(2,3D) through a pathway that may differ from that proposed for DBT. The mRNA expression of *Atf6*, *Txnip* and *Chop* were upregulated in beta cells exposed to BNT(2,3D) at the 1μM dose. However, BNT(2,3D) increased ROS production at 1nM, with no changes in ROS production observed at 1μM when compared to the controls. Therefore, neither ROS accumulation nor increased glucose uptake appear to contribute to the induction of ER stress in beta cells exposed to BNT(2,3D), however the pathway through which BNT(2,3D) may induce ER stress in beta cells has yet to be elucidated.

4.4 Some S-HACs Induce Cell Senescence

BNT(2,3D), but not DBT, upregulated mRNA expression of *p21* and significantly induced cellular senescence in the treated beta cells; however, mRNA expression of *p53* was not upregulated by either S-HAC suggesting a P53-independent pathway mediating the observed increase in senescence. Interestingly, a growing body of research is showing that P21 activation can occur independent of P53 activation, as demonstrated using P53-knockout mice (Megyesi et al. 1996). Various P53-independent pathways have been proposed. For example, TGFβ receptors I and II are expressed in adult beta cells, and activation of these receptors induces a signaling pathway which has been shown to affect beta cell proliferation and beta cell function (Jiang et al. 2018). TGFβ can induce cell senescence that is P53-independent and is associated with increased intracellular ROS production (Senturk et al. 2010). Interestingly, BNT(2,3D) at the 1nM dose significantly increased ROS production and induced cell senescence in the exposed beta cells.

Thus, it is possible that S-HACs may be inducing cell senescence in the beta cells through activation of the TGFβ pathway, which also induces ROS accumulation.

Alongside this, a 2011 study conducted by Prieur and colleagues has shown that cellular senescence can be induced without the generation of DNA damage nor the activation of P53 (Prieur et al. 2011). Senescence was induced by downregulating the activity of p300 histone acetyltransferase (P300 HAT) enzymes which resulted in cell cycle arrest at the G2/M phases (Prieur et al. 2011). P300 HAT enzymes are important in regulating cell growth and cell survival in the body, including in pancreatic beta cells, and exposure to diesel exhaust particles can regulate its activity (Prieur et al. 2011; Cao et al. 2007). Therefore, S-HACs may be capable of altering P300 HAT enzyme activity to consequently induce cellular senescence in exposed beta cells.

Beta cells exposed to 1nM of BNT(2,3D) expressed higher levels of the genes encoding the antiapoptotic protein BCL2 and the senescence associated enzyme GLB1, two key features of senescent cells. Furthermore, histochemical staining for beta-galactosidase expression in INS-1E cells showed increased expression of this protein in beta cells exposed to 1nM of BNT(2,3D) compared to controls, which is consistent with the results from the qPCR analysis.

Upon induction of cellular senescence in the beta cells, upregulation in mRNA expression of the SASP inflammatory marker *Serpine1* is observed in beta cells exposed to 1nM of BNT(2,3D). This suggests that the senescent beta cells have remained metabolically active and maybe inducing an inflammatory response to aid in rapidly spreading cellular senescence across beta cells. Therefore, BNT(2,3D) may be capable of inducing and rapidly spreading senescence in pancreatic tissues at doses that reflect non-occupational exposure levels.

The induction of cellular senescence in pancreatic beta cells can yield detrimental outcomes in the pancreatic islet and in the body as a whole. For example, the pro-inflammatory state of senescent beta cells can contribute to the induction of systemic insulin resistance (Akbari & Hassan-Zadeh 2018). The increased production of inflammatory proteins in the senescent beta cells can also impair the function of insulin exocytosis machinery, thereby impairing insulin secretion (Choi et al. 2009). Therefore, cellular senescence in beta cells can induce insulin resistance and beta cell dysfunction, consequently leading to impaired glucose tolerance in the body (Choi et al. 2009; Larsen et al. 2007).

4.5 ER Stress, Senescence and RAGE

Activation of RAGE can alter beta cell function and induce cellular stress (Coughlan et al. 2011; Piperi et al. 2012). The simultaneous occurrence of cellular senescence and, potentially, ER stress in beta cells exposed to BNT(2,3D) suggests that BNT(2,3D) may have interacted with the AGE-associated receptor, RAGE, embedded in the plasma membrane of beta cells. S-HACs may bind to RAGE on the plasma membrane of the beta cell and increase glucose uptake (Coughlan et al. 2011). Intracellular ROS production may also be increased due to RAGE activation (Coughlan et al. 2011). Some of the generated H_2O_2 may diffuse into the ER and induce ER stress (Piperi et al. 2012). Increased protein folding, in response to ER stress, leads to further ROS production (Pluquet et al. 2014). The accumulation of H_2O_2 activates P21 which induces cell senescence (Liu et al. 2014). The ability of RAGE to induce cellular stress and cellular senescence provides another potential P53-independent pathway through which S-HACs may affect beta cell health and beta cell function, however this remains to be determined.

4.6 S-HACs May Not Impair Insulin Production

The mRNA expression of *Isl1*, which regulates insulin gene expression, was upregulated by BNT(2,3D) at 1nM and by DBT at 1nM and 1μM. However, neither BNT(2,3D) nor DBT at these doses upregulated the expression of *Ins2*, which encodes the insulin hormone, in the treated beta cells. Furthermore, none of these doses altered insulin content in the exposed beta cells.

Beta cells exposed to either S-HAC did not have consistent changes, nor exhibit deficits, in intracellular insulin content. Therefore, BNT(2,3D) and DBT may not alter insulin production in beta cells, despite increased glucose uptake. However, the rate at which the insulin is secreted might differ from non-treated cells. During insulin secretion only a fraction of the total insulin packed in each vesicle is released out of the cell and into the bloodstream, even when stimulated with high glucose concentrations (Weiss et al. 2014). Therefore, beta cells regulate insulin plasma concentrations based on the rate at which insulin is secreted from the beta cell, rather than the rate at which insulin is synthesized (Weiss et al. 2014).

BNT(2,3D) upregulated the mRNA expression of *Kcnj11* in beta cells at the 1μM dose. *Kcnj11* encodes KIR6.2, a component of the K_{ATP} channel (Wu et al. 2014). The closure of the K_{ATP} channel and the subsequent membrane depolarization that occurs is a crucial step in the secretion of insulin from the beta cell (Fridlyand & Philipson 2011). In fact, antidiabetic drugs such as sulfonylureas target *KCNJ11* expression to enhance the secretion of insulin (Wu et al. 2014). Therefore, by increasing glucose uptake and upregulating the expression of *Kcnj11* S-HACs, particularly BNT(2,3D), may induce membrane depolarization in the beta cell and potentially enhance insulin release.

4.7 The Power of the Low Dose

It is interesting to note that for many of the outcome measures in this thesis, the data display a non-monotonic dose-response in which the direction of the slope of the dose-response curve changes across the examined dose range (Lagarde et al. 2015). For example, a non-monotonic dose-response is evident in the data generated from the intracellular ROS and cell senescence experiments (see Figures 7 and 11 in Results section). Various mechanisms have been proposed to explain this phenomenon (Lagarde et al. 2015). One proposed mechanism is that high doses can induce receptor desensitization leading to attenuation or complete inhibition of effects normally elicited by the bound ligand; similar to the desensitization of insulin receptors during hyperinsulinemic conditions (Lagarde et al. 2015; Shanik et al. 2008). Another proposed mechanism relates to receptor selectivity (Lagarde et al. 2015). At a low dose, the compound may bind solely to a single designated receptor type; however, at higher doses the compound may bind to the same receptor along with other receptor types (Lagarde et al. 2015). Binding to additional receptor types may activate signalling pathways that counteract or mitigate the effects elicited by the signalling pathways activated by the single receptor type at the low dose (Lagarde et al. 2015). The non-monotonic dose-response is commonly observed by endocrine disrupting chemicals, including many PACs (Lagarde et al. 2015). The ability of S-HACs to induce effects at relatively low but environmentally relevant concentrations suggests the high potency of these compounds.

4.8 Implications for Communities Residing Near Oil and Gas Extraction Sites

While it is unclear whether S-HACs can impair insulin secretion in the beta cell, the results of this thesis demonstrate that S-HACs can generate cellular stress and induce cell senescence, leading to the premature aging of the beta cells. Therefore, S-HACs are potential beta cell

toxicants. S-HACs, as previously mentioned, are a class of PACs that are found abundantly in various oil and gas extraction sites, including the Alberta oil sands regions (Harner et al. 2018).

The presence of HACs, including S-HACs, in air, snow, precipitation and surface sediment samples collected from regions several kilometres away from extraction sites demonstrates the high volatility of these compounds and potential for exposure (Harner et al. 2018). Furthermore, PACs in general have been found at higher concentrations in liver, kidney and muscle tissues of moose, beaver and ducks caught in the Alberta oil sands region when compared to PAC concentrations in co-op beef (McClachlan 2014). Individuals in communities near oil and gas extraction sites can be exposed to S-HACs through their diet; for example through consumption of wild-caught meats such as moose, beaver, and duck which may be part of their regular or traditional diet (McClachlan 2014).

Furthermore, oil spills in active extraction sites can lead to substantially greater accumulation of PACs in animals which inhabit the regions impacted by the spills. For example, sea otters were one of the primary species affected by the Exxon Valdez oil spill in Prince William Sound, Alaska (Ballachey & Kloecker 1997). Liver samples extracted from sea otter carcases from Prince William Sound following the spill contained, on average, 50nM of DBT which is substantially higher than the 10pM – 10nM range of concentrations of DBT found in the river otter liver samples obtained from the Alberta oil sands region (Ballachey & Kloecker 1997). PAC accumulation in wildlife, particularly in wild-caught meats, and the presence of these persistent organic compounds in water sources and the atmosphere may be contributing factors to the high prevalence rates of T2D in many communities residing near oil and gas extraction sites. Developing a suitable protocol for measuring plasma S-HAC concentrations in

people can help quantitatively determine the degree to which humans are exposed to these potential beta cell toxicants, especially for communities near bitumen extraction sites.

CHAPTER 5 - FUTURE DIRECTIONS

5.1 Effect of S-HACs on Oxidative Damage

Both BNT(2,3D) and DBT significantly increased ROS production in the treated INS-1E cells, however neither S-HAC altered the mRNA expression of *p53*. While it has been demonstrated that ROS can upregulate *p21* mRNA expression in a P53-independent manner, it is still important to determine whether S-HACs induced oxidative damage in treated beta cells (Qiu et al. 1996). As previously discussed, mRNA expression of a target gene is not always an accurate reflection of its protein expression (Edfors et al. 2016). Therefore running an oxidative damage assay, in which oxidative DNA damage is detected by measuring the protein expression of an oxidative damage marker, would help clarify if the observed increase in ROS production led to oxidative damage or whether the antioxidant enzymes were induced at sufficient levels to offer protection from oxidative damage. If oxidative damage occurred following exposure to the test compounds this would also provide some clarity to our understanding of whether it was ROS or oxidative damage that induced cellular senescence in the BNT(2,3D) exposed beta cells.

Various oxidative damage markers exist that can be used to detect/measure oxidative DNA damage in the INS-1E cells exposed to the selected S-HACs. One commonly examined marker is γ-H2AX, which is generated through the phosphorylation of the histone variant H2AX during DNA damage (Gruosso et al. 2016). γ-H2AX plays an important role in the DNA damage response by securely positioning repair proteins at DNA damage sites and enhancing DNA damage signalling (Gruosso et al. 2016). Therefore, oxidative DNA damage increases γ-H2AX protein expression (Gruosso et al. 2016). There are many functional assays available for quantitatively measuring γ-H2AX levels. For example, immunofluorescence staining of γ-H2AX

can be performed to detect DNA damage sites in INS-1E cells treated with S-HACs and compare to non-treated INS-1E cells.

5.2 Effect of S-HACs on Mitochondrial Function

It has been previously observed that DBT not only increases ROS production in mammalian cells but as well lowers the mitochondrial membrane potential of the exposed cell, which is indicative of impaired mitochondrial function (Sarma et al. 2017). Since both BNT(2,3D) and DBT significantly increased ROS production in the beta cells, it is important to determine if these S-HACs can also impair mitochondrial activity in the beta cell. Alongside measuring mitochondrial membrane potential, another common method for examining mitochondrial activity is through measuring ATP and ADP production in the mitochondria. During oxidative phosphorylation, the electron transport chain generates a proton electrochemical gradient that drives the conversion of ADP to ATP by the ATP synthase enzyme (Fridlyand & Philipson 2011). This is the primary function of the mitochondria (Fridlyand & Philipson 2011). The ratio of ATP:ADP produced also regulates the closure of K_{ATP} channels which are important in stimulating the subsequent pulse-like release of insulin-packed vesicles from the beta cell (Skelin et al. 2010).

Bioluminescence can be used to detect and quantify ATP and ADP production and help determine whether the ratio of intracellular concentrations of ATP:ADP are altered by exposure to such S-HACs as BNT(2,3D) and DBT. The intent is to determine if the ability of S-HACs in inducing mitochondrial ROS production can also impair the mitochondrial activity of the exposed cell.

5.3 Effect of S-HACs on Insulin Secretion

It is evident that S-HACs do not impair insulin production, however it is unclear whether insulin secretion was altered by the S-HAC treatments. Impaired insulin secretion, specifically a loss of phase 1 insulin release, characterizes beta cell dysfunction (Leahy 2005). In this study, mRNA expression of *Kcnj11* was upregulated and glucose uptake was increased, suggesting increased membrane depolarization and potentially enhanced insulin release. In the body, increased secretion of insulin into the blood may lead to hyperinsulinemia (Shanik et al. 2008). Persistent stimulation of insulin receptors in target tissues may lead to reduced insulin sensitivity by these receptors and impair glucose uptake into those target tissues, potentially leading to chronic, post-prandial hyperglycemia (Shanik et al. 2008).

Insulin release can be measured in S-HAC exposed beta cells through assessing glucose-stimulated insulin secretion. INS-1E cells that have been pre-treated with BNT(2,3D) and DBT can be afterwards treated with high and low glucose concentrations. Insulin content in the collected media can then be measured by running an insulin ELISA such as the ultrasensitive rat insulin ELISA (Crystal Chem, Illinois, USA). This will help determine if S-HAC exposure alters the rate of insulin secretion in exposed beta cells.

CONCLUSION

S-HACs can increase ROS production in pancreatic beta cells and induce cellular stress. Glucose uptake was also increased, however it is unclear whether it is directly due to S-HAC exposure. Some S-HACs can also induce cellular senescence in response to the cellular stress. The accumulation of ROS in the beta cell and induction of a senescent state may alter important beta cell functions, including mitochondrial activity and insulin secretion that could lead to the development of T2D, an age-associated disease (Hameed et al. 2015). Furthermore, S-HACs are abundantly found in air, waterbodies, soils and sediments of oil extraction sites, and traces of these persistent organic pollutants have also been found in the tissues of wildlife inhabiting those regions. The presence of S-HACs in food sources and in the environment and the ability of S-HACs in inducing cellular stress suggests that S-HACs may potentially be novel beta cell toxicants that influence the rates of T2D in communities in close proximity to oil extraction sites.

REFERENCES

Abdel-Shafy, H. I., & Mansour, M. S. (2016). A review on polycyclic aromatic hydrocarbons: Source, environmental impact, effect on human health and remediation. *Egyptian Journal of Petroleum*, *25*(1), 107–123. doi: 10.1016/j.ejpe.2015.03.011

Akbari, M., & Hassan-Zadeh, V. (2018). IL-6 signalling pathways and the development of type 2 diabetes. *Inflammopharmacology*, *26*(3), 685–698. doi: 10.1007/s10787-018-0458-0

Al-Goblan, A., Al-Alfi, M., & Khan, M. (2014). Mechanism linking diabetes mellitus and obesity. *Diabetes, Metabolic Syndrome and Obesity: Targets and Therapy*, 587. https://doi.org/10.2147/DMSO.S67400

Asif, M., & Wenger, L. M. (2019). Heterocyclic aromatic hydrocarbon distributions in petroleum: A source facies assessment tool. *Organic Geochemistry*, *137*, 103896. doi: 10.1016/j.orggeochem.2019.07.005

Back, S. H., Scheuner, D., Han, J., Song, B., Ribick, M., Wang, J., Gildersleeve, R. D., Pennathur, S., & Kaufman, R. J. (2009). Translation attenuation through eIF2α phosphorylation prevents oxidative stress and maintains the differentiated state in beta cells. *Cell Metabolism*, *10*(1), 13–26. https://doi.org/10.1016/j.cmet.2009.06.002

Ballachey, B. E., & Kloecker, K. A. (1997). *Hydrocarbons in hair, livers, and intestines of sea otters (Enhydra lutris) found dead along the path of the Exxon Valdez oil spill* (Report MMS 6-3; Report). USGS Publications Warehouse. http://pubs.er.usgs.gov/publication/2002012

Barnes, P. J. (2015). Mechanisms of development of multimorbidity in the elderly. *European Respiratory Journal*, *45*(3), 790–806. doi: 10.1183/09031936.00229714

Baud, O. (2004). Glutathione Peroxidase-Catalase Cooperativity Is Required for Resistance to Hydrogen Peroxide by Mature Rat Oligodendrocytes. *Journal of Neuroscience*, *24*(7), 1531–1540. doi: 10.1523/JNEUROSCI.3989-03.2004

Beuckelaer, A. (1996). A closer examination on some parametric alternatives to the ANOVA F-test. *Statistical Papers*, *37*(4), 291–305. doi: 10.1007/BF02926110

Bhandary, B., Marahatta, A., Kim, H.-R., & Chae, H.-J. (2013). An Involvement of Oxidative Stress in Endoplasmic Reticulum Stress and Its Associated Diseases. *International Journal of Molecular Sciences*, *14*(1), 434–456. doi: 10.3390/ijms14010434

Brown, A. M. (2005). A new software for carrying out one-way ANOVA post hoc tests. *Computer Methods and Programs in Biomedicine*, *79*(1), 89–95. doi:10.1016/j.cmpb.2005.02.007

Burgos-Morón, Abad-Jiménez, Marañón, Iannantuoni, Escribano-López, López-Domènech, … Víctor. (2019). Relationship Between Oxidative Stress, ER Stress, and Inflammation in Type 2 Diabetes: The Battle Continues. *Journal of Clinical Medicine*, *8*(9), 1385. doi: 10.3390/jcm8091385

Cao, D., Bromberg, P. A., & Samet, J. M. (2007). COX-2 Expression Induced by Diesel Particles Involves Chromatin Modification and Degradation of HDAC1. *American Journal of Respiratory Cell and Molecular Biology*, *37*(2), 232–239. doi:10.1165/rcmb.2006-0449OC

Cersosimo, E., Triplitt, C., Solis-Herrera, C., Mandarino, L.J., & DeFronzo, R.A. (2018, February 27). Pathogenesis of Type 2 Diabetes Mellitus. Retrieved from https://www.ncbi.nlm.nih.gov/books/NBK279115/

Choi, D., Radziszewska, A., Schroer, S. A., Liadis, N., Liu, Y., Zhang, Y., Lam, P. P. L., Sheu, L., Hao, Z., Gaisano, H. Y., & Woo, M. (2009). Deletion of Fas in the pancreatic β-cells leads to enhanced insulin secretion. *American Journal of Physiology-Endocrinology and Metabolism*, *297*(6), E1304–E1312. doi: 10.1152/ajpendo.00217.2009

Coggins, C. R. E., Merski, J. A., & Oldham, M. J. (2011). A comprehensive evaluation of the toxicology of cigarette ingredients: Heterocyclic nitrogen compounds. *Inhalation Toxicology*, *23 Suppl 1*, 84–89. https://doi.org/10.3109/08958378.2010.545841

Coughlan, M. T., Yap, F. Y. T., Tong, D. C. K., Andrikopoulos, S., Gasser, A., Thallas-Bonke, V., … Forbes, J. M. (2011). Advanced Glycation End Products Are Direct Modulators of β-Cell Function. *Diabetes*, *60*(10), 2523–2532. doi: 10.2337/db10-1033

Drews, G., Krippeit-Drews, P. & Dufer, M. (2010). Oxidative stress and beta-cell dysfunction. *European Journal of Physiology*, *460*, 703-718.

Du, Y., Liu, J., Zhu, Y., Yuan, X., Gao, J., Cheng, J., & Yan, X. (2019). Diesel exhaust particles induce toxicity to beta cells by suppressing miR-140-5p. *International Journal of Clinical and Experimental Pathology*, *12*(8), 2858–2866.

Edfors, F., Danielsson, F., Hallström, B. M., Käll, L., Lundberg, E., Pontén, F., Forsström, B., & Uhlén, M. (2016). Gene-specific correlation of RNA and protein levels in human cells and tissues. *Molecular Systems Biology*, *12*(10). doi: 10.15252/msb.20167144

Eisenträger, A., Brinkmann, C., Hollert, H., Sagner, A., Tiehm, A., & Neuwoehner, J. (2008). Heterocyclic Compounds: Toxic Effects Using Algae, Daphnids and the Salmonella/Microsome Test Taking Methodical Quantitative Aspects into Account. *Environmental Toxicology and Chemistry*, 1. doi: 10.1897/07-201

Eizirik D. L., Cardozo, A. K., & Cnop, M. (2007). The Role for Endoplasmic Reticulum Stress in Diabetes Mellitus. *Endocrine Reviews*, *29*(1), 42–61. doi: 10.1210/er.2007-0015

Ellingsgaard, H., Ehses, J. A., Hammar, E. B., Van Lommel, L., Quintens, R., Martens, G., Kerr-Conte, J., Pattou, F., Berney, T., Pipeleers, D., Halban, P. A., Schuit, F. C., & Donath, M.

Y. (2008). Interleukin-6 regulates pancreatic alpha-cell mass expansion. *Proceedings of the National Academy of Sciences*, *105*(35), 13163–13168. doi: 10.1073/pnas.0801059105

Fabricio, G., Malta, A., Chango, A., & Mathias, P. C. D. F. (2016). Environmental Contaminants and Pancreatic Beta-Cells. *Journal of Clinical Research in Pediatric Endocrinology*, *8*(3). doi: 10.4274/jcrpe.2812

Fridlyand, L. E., & Phillipson, L. H. (2011). Mechanisms of glucose sensing in the pancreatic β-cell. *Islets*, *3*(5), 224-230. doi:10.4161/isl.3.5.16409

Gruosso, T., Mieulet, V., Cardon, M., Bourachot, B., Kieffer, Y., Devun, F., Dubois, T., Dutreix, M., Vincent-Salomon, A., Miller, K. M., & Mechta-Grigoriou, F. (2016). Chronic oxidative stress promotes H2AX protein degradation and enhances chemosensitivity in breast cancer patients. *EMBO Molecular Medicine*, *8*(5), 527–549. https://doi.org/10.15252/emmm.201505891

Hameed, I., Masoodi, S.R., Mir, S.A., Nabi, M., Ghazanfar, K. & Ganai, B.A. (2015). Type 2 diabetes mellitus: From a metabolic disorder to an inflammatory condition. *World Journal of Diabetes*, *6(4)*, 598-612.

Harner, T., Rauert, C., Muir, D., Schuster, J. K., Hsu, Y.-M., Zhang, L., Marson, G., Watson, J. G., Ahad, J., Cho, S., Jariyasopit, N., Kirk, J., Korosi, J., Landis, M. S., Martin, J. W., Zhang, Y., Fernie, K., Wentworth, G. R., Wnorowski, A., … Wang, X. (2018). Air synthesis review: Polycyclic aromatic compounds in the oil sands region. *Environmental Reviews*, *26*(4), 430–468. doi: 10.1139/er-2018-0039

Hasnain, S. Z., Prins, J. B., & McGuckin, M. A. (2016). Oxidative and endoplasmic reticulum stress in β-cell dysfunction in diabetes. *Journal of Molecular Endocrinology*, *56*(2), R33–R54. doi:10.1530/JME-15-0232

Hectors, T.L.M., Vanparys, C., van der Ven, K., Martens, G. A., Jorens, P. G., Van Gaal, L. F., Covaci, A., De Coen, W., & Blust, R. (2011). Environmental pollutants and type 2 diabetes: a review of mechanisms that can disrupt beta cell function. *Diabetologia*, *54*, 1273-1290.

Houlden, R. L. (2018). Introduction. *Canadian Journal of Diabetes*, *42*. doi: 10.1016/j.jcjd.2017.10.001

IARC. (2013). *Bitumens and bitumen emissions, and some N-ands S-heterocyclic polycyclic aromatic hydrocarbons*. Lyon, France.

IDF. (2019). Diabetes Atlas 9th Edition 2019 [Digital image]. Retrieved April 21, 2020, from https://diabetesatlas.org/en/resources/

Jacob, J., Schmoldt, A., Augustin, C., Raab, G., & Grimmer, G. (1991). Rat liver microsomal ring- and S-oxidation of thiaarenes with central or peripheral thiophene rings. *Toxicology, 68*(2), 181-194. doi:10.1016/0300-483x(91)90020-2

Jacob, J., Schmoldt, A. & Grimmer, G. (1986). The predominant role of s-oxidation in rat liver metabolism of thiaarenes. *Cancer Letters, 32,* 107-116.

Jiang, Y., Fischbach, S., & Xiao, X. (2018). The Role of the TGFβ Receptor Signaling Pathway in Adult Beta Cell Proliferation. *International Journal of Molecular Sciences, 19*(10). doi: 10.3390/ijms19103136

Kasai, S., Shimizu, S., Tatara, Y., Mimura, J., & Itoh, K. (2020). Regulation of Nrf2 by Mitochondrial Reactive Oxygen Species in Physiology and Pathology. *Biomolecules*, *10*(2), 320. doi: 10.3390/biom10020320

Khan, S. S., Shah, S. J., Klyachko, E., Baldridge, A. S., Eren, M., Place, A. T., Aviv, A., Puterman, E., Lloyd-Jones, D. M., Heiman, M., Miyata, T., Gupta, S., Shapiro, A. D., & Vaughan, D. E. (2017). A null mutation in *SERPINE1* protects against biological aging in humans. *Science advances*, *3*(11), eaao1617. doi: 10.1126/sciadv.aao1617

Kim, M.-K., Kim, H.-S., Lee, I.-K., & Park, K.-G. (2012). Endoplasmic Reticulum Stress and Insulin Biosynthesis: A Review. *Experimental Diabetes Research, 2012*, 1–7. doi: 10.1155/2012/509437

Kim, Y. H., Lee, Y. S., Lee, D. H., & Kim, D. S. (2016). Polycyclic aromatic hydrocarbons are associated with insulin receptor substrate 2 methylation in adipose tissues of Korean women. *Environmental Research, 150,* 47–51. doi: 10.1016/j.envres.2016.05.043

Lagarde, F., Beausoleil, C., Belcher, S. M., Belzunces, L. P., Emond, C., Guerbet, M., & Rousselle, C. (2015). Non-monotonic dose-response relationships and endocrine disruptors: A qualitative method of assessment. *Environmental Health, 14*. doi: 10.1186/1476-069X-14-13

Larsen, C. M., Faulenbach, M., Vaag, A., Volund, A., Ehses, J. A., Seifert, B., … Donath, M. Y. (2007). Interleukin-1–Receptor Antagonist in Type 2 Diabetes Mellitus. *New England Journal of Medicine, 357*(3), 302–303. doi: 10.1056/nejmc071324

Leahy, J. L. (2005). Pathogenesis of Type 2 Diabetes Mellitus. *Archives of Medical Research, 36*(3), 197–209. https://doi.org/10.1016/j.arcmed.2005.01.003

Lee, B. Y., Han, J. A., Im, J. S., Morrone, A., Johung, K., Goodwin, E. C., … Hwang, E. S. (2006). Senescence-associated β-galactosidase is lysosomal β-galactosidase. *Aging Cell*, *5*(2), 187–195. doi: 10.1111/j.1474-9726.2006.00199.x

Li, C., Singh, A., Klamerth, N., McPhedran, K., Chelme-Ayala, P., Belosevic, M. & Gamal El-Din, M. (2014). Synthesis of toxicological behaviour of oil sands process-affected water

constituents. Oil Sands Research and Information Network, University of Alberta, School of Energy and the Environment. Edmonton, Alberta. 101 pp.

Lin, Y., Qiu, X., Yu, N., Yang, Q., Araujo, J.A. & Zhu, Y. (2016). Urinary Metabolites of Polycyclic Aromatic Hydrocarbons and the Association with Lipid Peroxidation: A Biomarker-Based Study between Los Angeles and Beijing. *Environmental Science & Technology*, *50*, 3738-3745.

Liu, J., Huang, K., Cai, G.-Y., Chen, X.-M., Yang, J.-R., Lin, L.-R., … He, Y.-N. (2014). Receptor for advanced glycation end-products promotes premature senescence of proximal tubular epithelial cells via activation of endoplasmic reticulum stress-dependent p21 signaling. *Cellular Signalling*, *26*(1), 110–121. doi: 10.1016/j.cellsig.2013.10.002

Livak, K. J., & Schmittgen, T. D. (2001). Analysis of relative gene expression data using real-time quantitative PCR and the 2(-Delta Delta C(T)) Method. *Methods (San Diego, Calif.)*, *25*(4), 402–408. doi: 10.1006/meth.2001.1262

López-García, J., Lehocký, M., Humpolíček, P., & Sáha, P. (2014). HaCaT Keratinocytes Response on Antimicrobial Atelocollagen Substrates: Extent of Cytotoxicity, Cell Viability and Proliferation. *Journal of Functional Biomaterials*, *5*(2), 43–57. https://doi.org/10.3390/jfb5020043

Mahbobi, M., & Tiemann, T. K. (2015). *Introductory Business Statistics with Interactive Spreadsheets—1st Canadian Edition*. BCcampus. https://opentextbc.ca/introductorybusinessstatistics/

McLachlan, S. M. (2014). *"Water is a living thing" Environmental and Human Health Implications of the Athabasca Oil Sands for the Mikisew Cree First Nation and Athabasca Chipewyan First Nation in Northern Alberta.* (p. 242). Environmental Conservation Laboratory, University of Manitoba.

Megyesi, J., Udvarhelyi, N., Safirstein, R. L., & Price, P. M. (1996). The p53-independent activation of transcription of p21 WAF1/CIP1/SDI1 after acute renal failure. *American Journal of Physiology-Renal Physiology*, *271*(6). doi: 10.1152/ajprenal.1996.271.6.f1211

Miki, A., Ricordi, C., Sakuma, Y., Yamamoto, T., Misawa, R., Mita, A., Molano, R. D., Vaziri, N. D., Pileggi, A., & Ichii, H. (2018). Divergent antioxidant capacity of human islet cell subsets: A potential cause of beta-cell vulnerability in diabetes and islet transplantation. *PLoS ONE*, *13*(5). doi: 10.1371/journal.pone.0196570

Mossner, S.G. & Wise, S.A. (1999). Determination of polycyclic aromatic sulfur heterocycles in fossil fuel-related samples. *Analytical Chemistry, 71,* 58-69.

Net, S., El-Osmani, R., Prygiel, E., Rabodonirina, S., Dumoulin, D. & Ouddane, B. (2015). Overview of persistent organic pollution (HACs, Me-HACs and PCBs) in freshwater sediments from Northern France. *Journal of Geochemical Exploration*, *148*, 181-188.

Pallepati, P., & Averill-Bates, D. A. (2011). Activation of ER stress and apoptosis by hydrogen peroxide in HeLa cells: Protective role of mild heat preconditioning at 40°C. *Biochimica et Biophysica Acta (BBA) - Molecular Cell Research*, *1813*(12), 1987–1999. doi: 10.1016/j.bbamcr.2011.07.021

Piperi, C., Adamopoulos, C., Dalagiorgou, G., Diamanti-Kandarakis, E., & Papavassiliou, A. G. (2012). Crosstalk between Advanced Glycation and Endoplasmic Reticulum Stress: Emerging Therapeutic Targeting for Metabolic Diseases. *The Journal of Clinical Endocrinology & Metabolism*, *97*(7), 2231–2242. doi: 10.1210/jc.2011-3408

Pluquet, O., Pourtier, A., & Abbadie, C. (2014). The unfolded protein response and cellular senescence. A Review in the Theme: Cellular Mechanisms of Endoplasmic Reticulum Stress Signaling in Health and Disease. *American Journal of Physiology-Cell Physiology*, *308*(6). doi: 10.1152/ajpcell.00334.2014

Prieur, A., Besnard, E., Babled, A., & Lemaitre, J.-M. (2011). p53 and p16INK4A independent induction of senescence by chromatin-dependent alteration of S-phase progression. *Nature Communications*, *2*(1). doi: 10.1038/ncomms1473

Public Health Agency of Canada. (2019, December 9). Diabetes in Canada. Retrieved May 14, 2020, from https://www.canada.ca/en/public-health/services/publications/diseases-conditions/diabetes-canada-highlights-chronic-disease-surveillance-system.html

Punthakee, Z., Goldenberg, R., & Katz, P. (2018). Definition, Classification and Diagnosis of Diabetes, Prediabetes and Metabolic Syndrome. *Canadian Journal of Diabetes*, *42*. doi: 10.1016/j.jcjd.2017.10.003

Qiu, X., Forman, H. J., Schönthal, A. H., & Cadenas, E. (1996). Induction of p21 Mediated by Reactive Oxygen Species Formed during the Metabolism of Aziridinylbenzoquinones by HCT116 Cells. *Journal of Biological Chemistry*, *271*(50), 31915–31921. doi: 10.1074/jbc.271.50.31915

Reynolds, P. R., Wasley, K. M., & Allison, C. H. (2011). Diesel Particulate Matter Induces Receptor for Advanced Glycation End-Products (RAGE) Expression in Pulmonary Epithelial Cells, and RAGE Signaling Influences NF-κB–Mediated Inflammation. *Environmental Health Perspectives*, *119*(3), 332–336. doi: 10.1289/ehp.1002520

Rincheval, V., Renaud, F., Lemaire, C., Godefroy, N., Trotot, P., Boulo, V., … Vayssière, J.-L. (2002). Bcl-2 can promote p53-dependent senescence versus apoptosis without affecting the G1/S transition. *Biochemical and Biophysical Research Communications*, *298*(2), 282–288. doi: 10.1016/s0006-291x(02)02454-3

Sarma, S. N., Blais, J. M., & Chan, H. M. (2017). Neurotoxicity of alkylated polycyclic aromatic compounds in human neuroblastoma cells. *Journal of Toxicology and Environmental Health, Part A, 80*(5), 285–300. doi: 10.1080/15287394.2017.1314840

Schumann, D. M., Maedler, K., Franklin, I., Konrad, D., Storling, J., Boni-Schnetzler, M., Gjinovci, A., Kurrer, M. O., Gauthier, B. R., Bosco, D., Andres, A., Berney, T., Greter, M., Becher, B., Chervonsky, A. V., Halban, P. A., Mandrup-Poulsen, T., Wollheim, C. B., & Donath, M. Y. (2007). The Fas pathway is involved in pancreatic beta cell secretory function. *Proceedings of the National Academy of Sciences, 104*(8), 2861–2866. doi: 10.1073/pnas.0611487104

Seino, Y., Nanjo, K., Tajima, N., Kadowaki, T., Kashiwagi, A., Araki, E., … Ueki, K. (2010). Report of the Committee on the Classification and Diagnostic Criteria of Diabetes Mellitus. *Journal of Diabetes Investigation, 1*(5), 212–228. doi: 10.1111/j.2040-1124.2010.00074.x

Senturk, S., Mumcuoglu, M., Gursoy-Yuzugullu, O., Cingoz, B., Akcali, K. C., & Ozturk, M. (2010). Transforming growth factor-beta induces senescence in hepatocellular carcinoma cells and inhibits tumor growth. *Hepatology, 52*(3), 966–974. doi: 10.1002/hep.23769

Shanik, M. H., Xu, Y., Skrha, J., Dankner, R., Zick, Y., & Roth, J. (2008). Insulin Resistance and Hyperinsulinemia: Is hyperinsulinemia the cart or the horse? *Diabetes Care, 31*(Supplement 2). doi: 10.2337/dc08-s264

Silva-Veiga, F. M., Rachid, T. L., de Oliveira, L., Graus-Nunes, F., Mandarim-de-Lacerda, C. A., & Souza-Mello, V. (2018). GW0742 (PPAR-beta agonist) attenuates hepatic endoplasmic reticulum stress by improving hepatic energy metabolism in high-fat diet fed mice. *Molecular and Cellular Endocrinology, 474*, 227–237. doi: 10.1016/j.mce.2018.03.013

Skelin, M., Rupnik, M. & Cencic, A. (2010). Pancreatic beta cell lines and their applications in diabetes mellitus research. *ALTEX, 27*, 105-113.

Tavana, O., & Zhu, C. (2011). Too many breaks (brakes): Pancreatic β-cell senescence leads to diabetes. *Cell Cycle, 10*(15), 2471–2484. doi: 10.4161/cc.10.15.16741

Tong, X., Chaudhry, Z., Lee, C.-C., Bone, R. N., Kanojia, S., Maddatu, J., Sohn, P., Weaver, S. A., Robertson, M. A., Petrache, I., Evans-Molina, C., & Kono, T. (2020). Cigarette smoke exposure impairs β-cell function through activation of oxidative stress and ceramide accumulation. *Molecular Metabolism, 37*, 100975. doi: 10.1016/j.molmet.2020.100975

van der Spoel, A., Bonten, E., & Dazzo, A. (2000). Processing of Lysosomal β-Galactosidase. *Journal of Biological Chemistry, 275*(14), 10035–10040. doi: 10.1074/jbc.275.14.10035

Wang, J., Gu, W., & Chen, C. (2018). Knocking down Insulin Receptor in Pancreatic Beta Cell lines with Lentiviral-Small Hairpin RNA Reduces Glucose-Stimulated Insulin Secretion via Decreasing the Gene Expression of Insulin, GLUT2 and Pdx1. *International Journal of Molecular Sciences*, *19*(4). doi: 10.3390/ijms19040985

Weiss, M., Steiner, D. F., & Philipson, L. H. (2014). Insulin Biosynthesis, Secretion, Structure, and Structure-Activity Relationships. In K. R. Feingold, B. Anawalt, A. Boyce, G. Chrousos, K. Dungan, A. Grossman, J. M. Hershman, G. Kaltsas, C. Koch, P. Kopp, M. Korbonits, R. McLachlan, J. E. Morley, M. New, L. Perreault, J. Purnell, R. Rebar, F. Singer, D. L. Trence, … D. P. Wilson (Eds.), *Endotext*. MDText.com, Inc. http://www.ncbi.nlm.nih.gov/books/NBK279029/

Williams, P. T., Bartle, K. D., & Andrews, G. E. (1986). The relation between polycyclic aromatic compounds in diesel fuels and exhaust particulates. *Fuel*, *65*(8), 1150–1158. doi: 10.1016/0016-2361(86)90184-5

Wu, Y., Ding, Y., Tanaka, Y. & Zhang, W. (2014). Risk factors contributing to type 2 diabetes and recent advances in the treatment and prevention. *International Journal of Medical Sciences*, *11*, 1185-1200. doi: 10.7150/ijms.10001

Yang, L., Li, M., Wang, T. & Shi, Y. (2016). Dibenzothiophenes and benzonaphthothiophenes in oils, and their application in identifying oil filling pathways in Eocene lacustrine clastic reservoirs in the Beibuwan Basin, South China Sea. *Journal of Petroleum Science and Engineering*, *146*, 1026-1036.

Ye, Z., Liu, G., Guo, J., & Su, Z. (2018). Hypothalamic endoplasmic reticulum stress as a key mediator of obesity-induced leptin resistance: Obesity, leptin resistance and ER stress. *Obesity Reviews*, *19*(6), 770–785. doi: 10.1111/obr.12673

Yoon, S., Bhatt, S. D., Lee, W., Lee, H. Y., Jeong, S. Y., Baeg, J.-O., & Lee, C. W. (2009). Separation and characterization of bitumen from Athabasca oil sand. *Korean Journal of Chemical Engineering*, *26*(1), 64–71. doi: 10.1007/s11814-009-0011-3

Xiong, Q.-Y., Yu, C., Zhang, Y., Ling, L., Wang, L., & Gao, J.-L. (2017). Key proteins involved in insulin vesicle exocytosis and secretion. *Biomedical Reports*, *6*(2), 134–139. doi: 10.3892/br.2017.839

Zorova, L. D., Popkov, V. A., Plotnikov, E. Y., Silachev, D. N., Pevzner, I. B., Jankauskas, S. S., Babenko, V. A., Zorov, S. D., Balakireva, A. V., Juhaszova, M., Sollott, S. J., & Zorov, D. B. (2018). Mitochondrial membrane potential. *Analytical Biochemistry*, *552*, 50–59. doi: 10.1016/j.ab.2017.07.009

APPENDICES

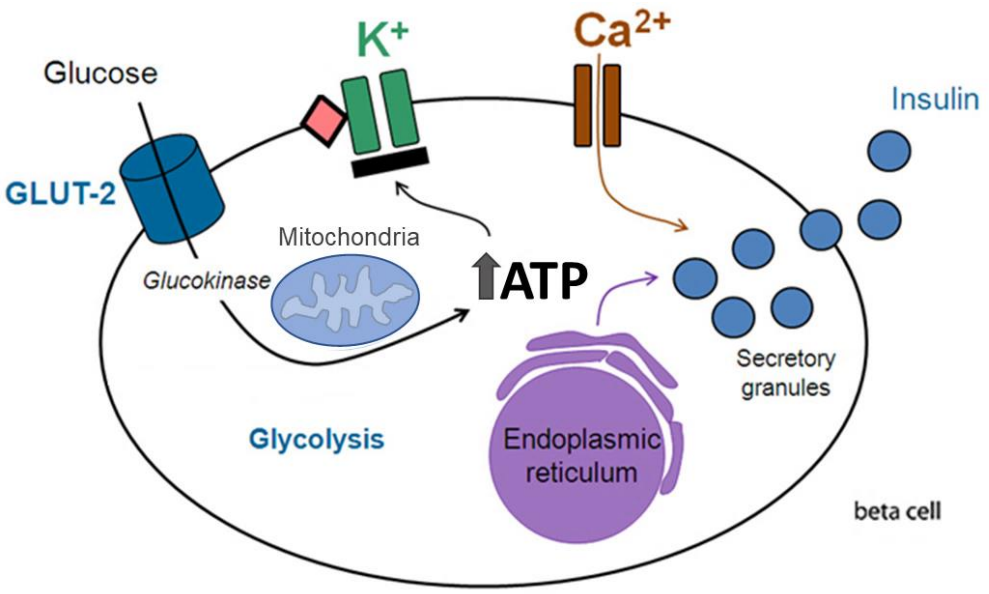

Appendix 1. Glucose-induced insulin secretion in the pancreatic beta cell. Figure obtained and adapted from Henzen 2012.

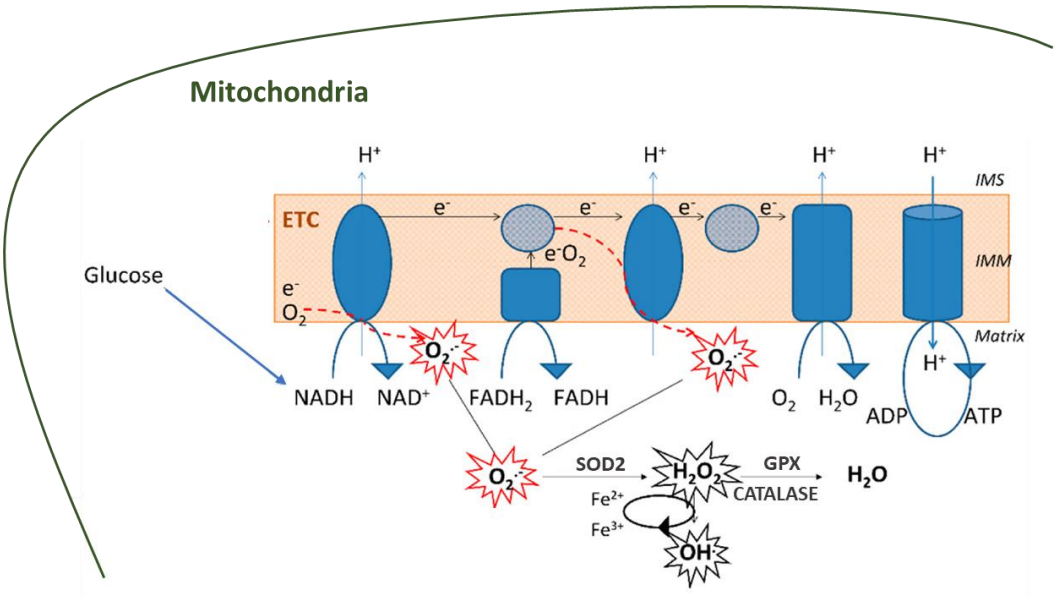

Appendix 2. Glucose uptake and mitochondrial generation of ROS. Figure obtained and adapted from Burgos-Moron et al. 2019.

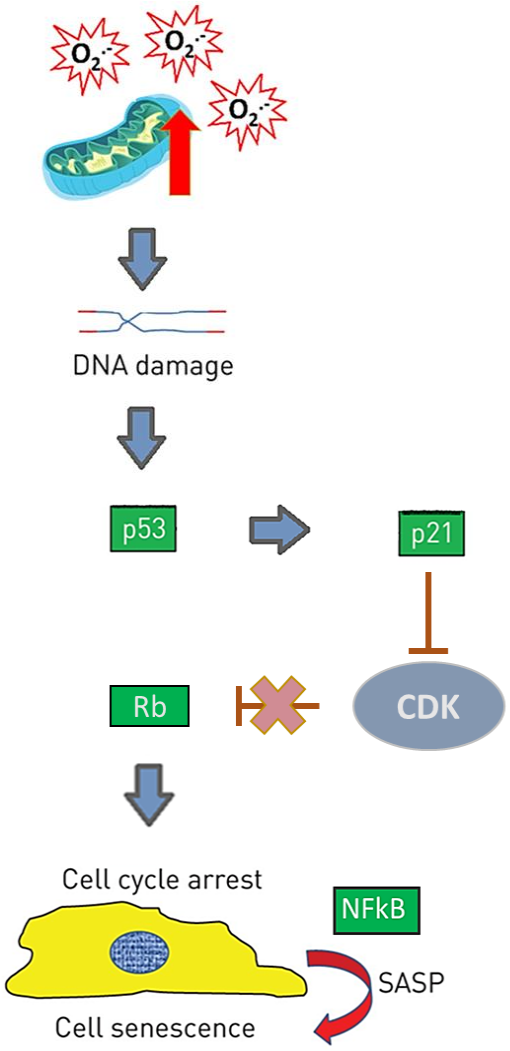

Appendix 3. The association between ROS accumulation and cellular senescence. Figure obtained and adapted from Barnes 2015.

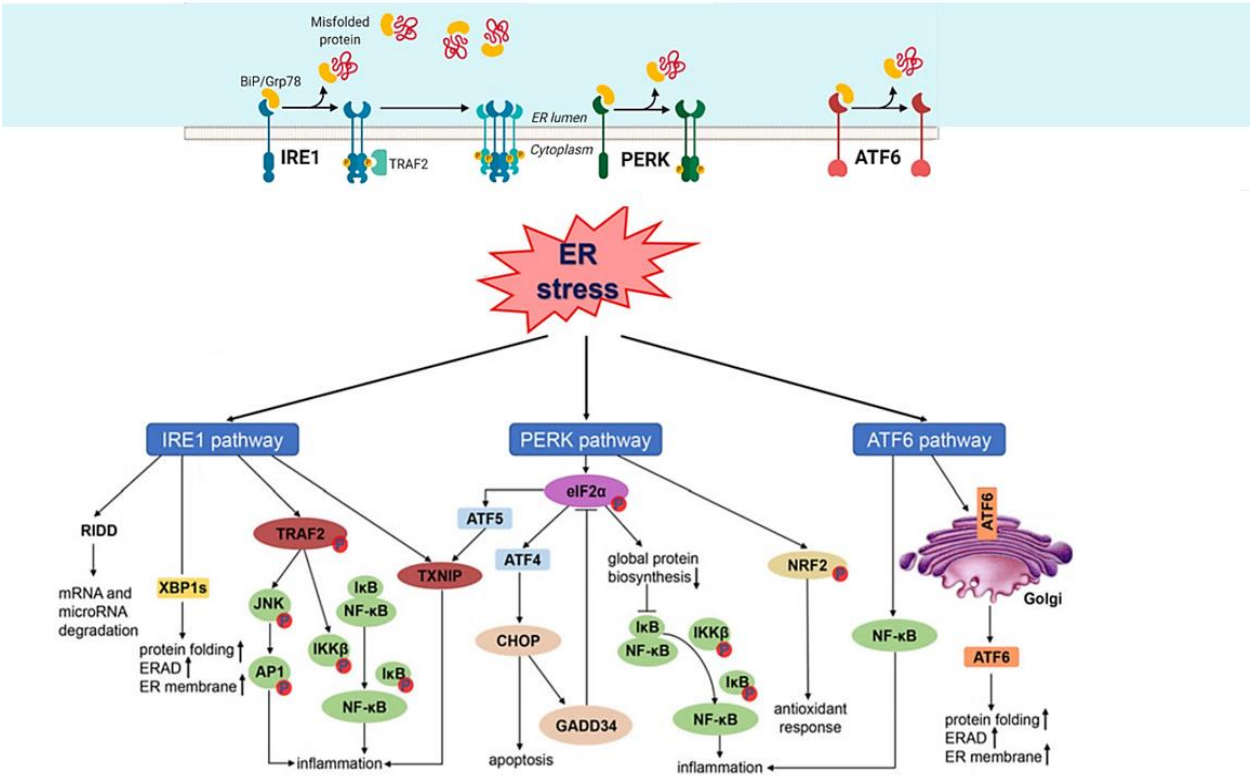

Appendix 4. ER stress and its induction of the unfolded protein response which is comprised of three transmembrane proteins (IRE1, PERK and ATF6) and their associated signalling pathways. Figure obtained and adapted from Ye et al. 2018.

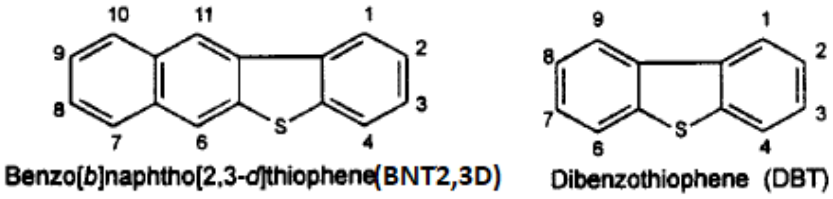

Appendix 5. 2D molecular structures of benzo[b]naphtho[2,3-d]thiophene (molecular mass: 234.32g/mol) and dibenzothiophene (molecular mass: 184.26g/mol). Figure obtained and adapted from Mossner & Wise 1999.

Primer Name	Primer Type	Function	Primer Sequence
Glut2	Target gene	Glucose uptake	Fwd: GCAATATCCTCCCTCCAGCC Rev: TGCAGGCACAACTCCCTTAG
Gck	Target gene	Glycolysis	Fwd: GATGCCAGAGGTTAGAGCCC Rev: GGTCAGGGACCTGAGTGTTG
Nrf2	Target gene	Regulates antioxidant activity	Fwd: ATTTGTAGATGACCATGAGTCGC Rev: TGTCCTGCTGTATGCTGCTT
Sod2	Target gene	Antioxidant activity in mitochondria	Fwd: ATTGCCGCCTGCTCTAATCA Rev: CTCCCACACATCAATCCCCA
Catalase	Target gene	Antioxidant activity in mitochondria	Fwd: CTGACACAGTTCGTGACCCT Rev: GTTTCCCACAAGGTCCCAGT
Gpx	Target gene	Antioxidant activity in mitochondria	Fwd: CCTGCCTTCAAATACCTAACCC Rev: TGTAATACGGGGCTTGATCTCC
p53	Target gene	Tumour suppression pathway	Fwd: AGCGACTACAGTTAGGGGGT Rev: ACAGTTATCCAGTCTTCAGGGG
p21	Target gene	Tumour suppression pathway	Fwd: GTGATATGTACCAGCCACAGG Rev: GAACAGGTCGGACATCACCA
Glb1	Target gene	Cellular senescence	Fwd: GGCTTTAACCTCGGGCGATA Rev: TGGTCAGGATGTTCCTTGGC
Bcl2	Target gene	Tumour suppressive properties	Fwd: GGATAACGGAGGCTGGGATG Rev: GCATGCTGGGGCCATATAGT
Nlrp3	Target gene	Regulates production and secretion of IL1β	Fwd: CACAACTCACCCAAGGAGGA Rev: ACAGGCAACATGAGGGTCTG
Il1b	Target gene	SASP	Fwd: GCAGTGTCACTCATTGTGGC Rev: AAGAAGGTGCTTGGGTCCTC
Serpine1	Target gene	SASP	Fwd: GCGAAACCCTCAGCATGTTC Rev: AATGTTGGTGATGGCGGAGA
Mcp1	Target gene	SASP	Fwd: CAGTTAATGCCCCACTCACCT Rev: CAGCTTCTTTGGGACACCTG
Il6	Target gene	SASP	Fwd: CCCACCAGGAACGAAAGTCA Rev: GCGGAGAGAAACTTCATAGCTGTT
Atf6	Target gene	Unfolded protein response	Fwd: GGATTTGATGCCTTGGGAGTCAGAC Rev: ATTTTTTTCTTTGGAGTCAGTCCAT
Grp78	Target gene	Unfolded protein response	Fwd: AACCCAGATGAGGCTGTAGCA Rev: ACATCAAGCAGAACCAGGTCAC
Txnip	Target gene	Unfolded protein response	Fwd: TGTTCCGTGTCCTGTGTCAG Rev: TCTCGGGTGGAGTGCTTAGA
Chop	Target gene	Unfolded protein response	Fwd: CCAGCAGAGGTCACAAGCAC Rev: CGCACTGACCACTCTGTTTC
Pdx1	Target gene	Regulates insulin gene expression	Fwd: CACCATGAATAGTGAGGAGCAG Rev: GATTAGCACTGAACTCTGGCAC
Mafa	Target gene	Regulates insulin expression	Fwd: AGGAGGAGGTCATCCGACTG Rev: CTTCTCGCTCTCCAGAATGTG
Isl1	Target gene	Regulates insulin gene expression	Fwd: CCAGGGGATGACAGGAACTC Rev: ACCTCAACTGGGTTAGCCTG
Ins2	Target gene	Encodes insulin	Fwd: GCGGCATCGTGGATCAGT

			Rev: GCCTAGTTGCAGTAGTTCTCCAGTT
Kcnj11	Target gene	Subunit of K_{ATP} channel	Fwd: GTCAGGGGCTCAGTAAGCAA Rev: ACTAGCTTCAGATGCCGACG
Gapdh	Housekeeping gene	_____	Fwd: TGGAGTCTACTGGCGTCTTCAC Rev: GGCATGGACTGTGGTCATGA
18s	Housekeeping gene	_____	Fwd: GCGATGCGGCGGCGTTAT Rev: AGACTTTGGTTTCCCGGAAGC

Appendix 6. List of selected target genes and housekeeping genes with description of function and primer sequences.